NATIONAL AERONAUTICS AND SPACE ADMINISTRATION

Technical Report 32-1500

Final Report on RF Voltage Breakdown in Coaxial Transmission Lines

R. Woo

JET PROPULSION LABORATORY
CALIFORNIA INSTITUTE OF TECHNOLOGY
PASADENA, CALIFORNIA

October 1, 1970

NATIONAL AERONAUTICS AND SPACE ADMINISTRATION

Technical Report 32-1500

Final Report on RF Voltage Breakdown in Coaxial Transmission Lines

R. Woo

JET PROPULSION LABORATORY
CALIFORNIA INSTITUTE OF TECHNOLOGY
PASADENA, CALIFORNIA

October 1, 1970

PRECEDING PAGE BLANK NOT FILMED

Preface

The work described in this report was performed by the Telecommunications Division of the Jet Propulsion Laboratory.

Acknowledgment

The author is grateful to G. Voyles for his efforts in obtaining the experimental data.

Contents

Tables

Contents (contd)

Figures

Abstract

Because of its occurrence in components designed for operation in space, RF voltage breakdown has attracted considerable interest in recent years. Extensive studies have been made of RF voltage breakdown in the coaxial transmission line geometry; the results are summarized in this report. Using the principle of similarity and a minimum of experimental data, universal curves are constructed covering a wide range of experimental parameters. These data are sufficient to determine the power handling capability of any coaxial transmission lines likely to be encountered by a spacecraft design engineer.

Final Report on RF Voltage Breakdown in Coaxial Transmission Lines

I. Introduction

The subject of voltage breakdown has gained considerable interest in recent years because of its occurrence in components designed for operation in space (Refs. 1–5). For spacecraft components such as transmission lines and antennas, voltage breakdown results in a disruption or loss of communications. Permanent damage to the components may also result. In the *Ranger* program, voltage breakdown problems developed in the transmitting system which had a transmitting power of 60 W at a frequency of 960 MHz (Refs. 1–3). Therefore, a research study was undertaken at the Jet Propulsion Laboratory to investigate voltage breakdown in the coaxial transmission line geometry. This particular geometry was selected for study not only because of the *Ranger* problems but also its common use in many RF systems. This report reviews and summarizes the results of this study.

II. Background

In its normal state, a gas is almost a perfect insulator. If a voltage is applied to a pair of electrodes and gradually increased, a point will be reached at which the intermediary gas will conduct. The result is a short-circuit condition. The transition from insulating to conducting state is called electrical or voltage breakdown and represents a subject that has been widely studied (Ref. 6). It is obvious that both RF and dc voltages can cause breakdown. This report concerns only RF voltage breakdown.

Voltage breakdown occurs when the generation of electrons exceeds the removal of electrons from the intermediary gas. In the case of RF voltage breakdown, the two main electron generation mechanisms are: ionization of the gas by electron collision, and secondary electron emission from the electrodes. Removal mechanisms include diffusion, drift, recombination, and attachment. These various electron production and loss mechanisms are discussed in Refs. 7 and 8. At pressures sufficiently low that the electron mean free path is longer than the electrode separation distance, the primary electron generation mechanism is secondary emission. This particular breakdown phenomenon is known as multipacting (Refs. 9 and 10), and generally occurs at pressures lower than 10^{-2} torr; the exact pressures below which multipacting occurs for various cases will be given later in this report. Multipacting breakdown is also discussed in Section III. At higher pressures, when the electron mean free path becomes shorter than the electrode separation distance, ionization by electron collision is the dominant electron production mechanism. For this reason, this type of breakdown will be termed ionization breakdown. Ionization breakdown is discussed in Section IV.

In preparing this document, a limited amount of background information on the breakdown phenomena is supplied to enable the reader to use the results intelligently. For the benefit of those seeking a more thorough understanding and a more complete survey of the field, two excellent accounts of RF or high-frequency voltage breakdown are given by Brown (Ref. 11) and Francis (Ref. 12). Reference 12 is especially useful because it contains a bibliography covering most work performed prior to the late fifties. More recently, MacDonald (Ref. 13) has written a book covering ionization breakdown with an emphasis on microwave frequencies and excluding multipacting. Because of the differences in the mechanisms involved, breakdown occurs more easily for RF than dc. An excellent discussion and comparison of dc and RF breakdown is given in Refs. 14 and 15.

III. Multipacting Breakdown

A. Description of Multipacting Mechanism

Multipacting breakdown is a secondary electron resonance breakdown (Refs. 7–12). It has occurred not only in RF components designed for operation in space, but in klystrons (Ref. 16), cyclotrons, and accelerators (Ref. 17) as well. On the constructive side, some multipacting devices have been built for practical applications (Ref. 18).

In multipacting breakdown, the pressure is sufficiently low so that the mean free path is longer than the electrode separation distance. Thus, electrons can readily travel between the electrodes without undergoing collisions with the gas molecules. When these electrons collide with the electrodes, they release secondary electrons provided that the primary electrons possess sufficient energy and that the electrode surfaces have a secondary emission coefficient greater than one. If this occurs as the electric field passes through zero, the reversed electric field will accelerate the electrons back across the gap. If the transit time of the electrons across the gap is one half cycle of the RF field, the secondary electrons formed by the initial electrons become primary electrons for the next half cycle to form another group of secondary electrons. In this way, large electron densities rapidly build up in the gap and breakdown results. It is clear that were the transit time of the electrons an odd integral multiple of one-half cycle, multipacting would also occur. These are referred to as the higher order multipacting modes (Ref. 10). The field configuration described is the simplest one that produces multipacting. Multipacting can also occur when dc or magnetic fields are superimposed (Ref. 12). The addition of a dc field, electric or magnetic, could give rise to the one-sided multipacting modes (Refs. 19 and 20). Such modes correspond to the case where secondary electrons are emitted from one electrode only.

A few important properties of multipacting should be pointed out. First of all, multipacting relies only on secondary electron emission from the electrodes. Thus, it is not dependent on the type of gas in which the breakdown takes place. Secondly, it should be clear from the breakdown mechanism that multipacting is independent of pressure. The only requirement on pressure is that it be sufficiently low so that the mean free path will be longer than the electrode separation distance. Multipacting is, therefore, one of the simplest breakdown mechanisms.

B. Scaling Relations for Multipacting

In order to predict multipacting, the electron trajectories must be known. Moreover, they must be appropriately related to the boundary conditions at the electrodes. Since electron trajectory solutions can readily be obtained for the parallel plates geometry, most multipacting studies have been restricted to that geometry (Refs. 11, 12, 19, 21, and 23). For electrode configurations where the fields are non-uniform, such as the coaxial transmission line, closed-form solutions of the electron trajectories are difficult, if not impossible, to obtain. Therefore, prediction of multipacting for such geometries becomes very difficult (Ref. 22).

To overcome these difficulties, it was decided to employ an approach totally different from conventional methods. Rather than solve the electron trajectories, the question was asked whether some scaling relations could be established for multipacting. In other words, under what conditions would multipacting data obtained for one set of experimental parameters apply to another set of experimental parameters. By studying the dimensionless Lorentz force equation which specifies the electron motion in the presence of electric and magnetic fields, scaling relations for multipacting were derived. One of the more important scaling results is the fact that breakdown voltage is invariant for a constant value of fd (f is frequency and d is the separation distance between inner and outer conductors), provided the characteristic impedance Z_0 is unchanged. This means that if the size of a transmission line is doubled and the frequency halved, the voltage at which breakdown occurs remains the same. Reference 22 provides details of the derivation of this and other scaling results.

The advantages in scaling laws are as follows: (1) the scope of an experimental investigation could be significantly reduced, (2) universal curves for predicting multipacting over a wide range of experimental parameters could be constructed, and (3) if the computer is employed to calculate electron trajectories, similar solutions need be obtained only once.

C. Coaxial 50-Ω Transmission Lines

Shown in Fig. 1 are various sets of experimental data for the 50 Ω coaxial line geometry. In this case, the ratio b/a (b and a are the radii of the outer and inner conductors, respectively) is 2.3. Data were obtained in a frequency range of 10–150 MHz, where lumped circuit

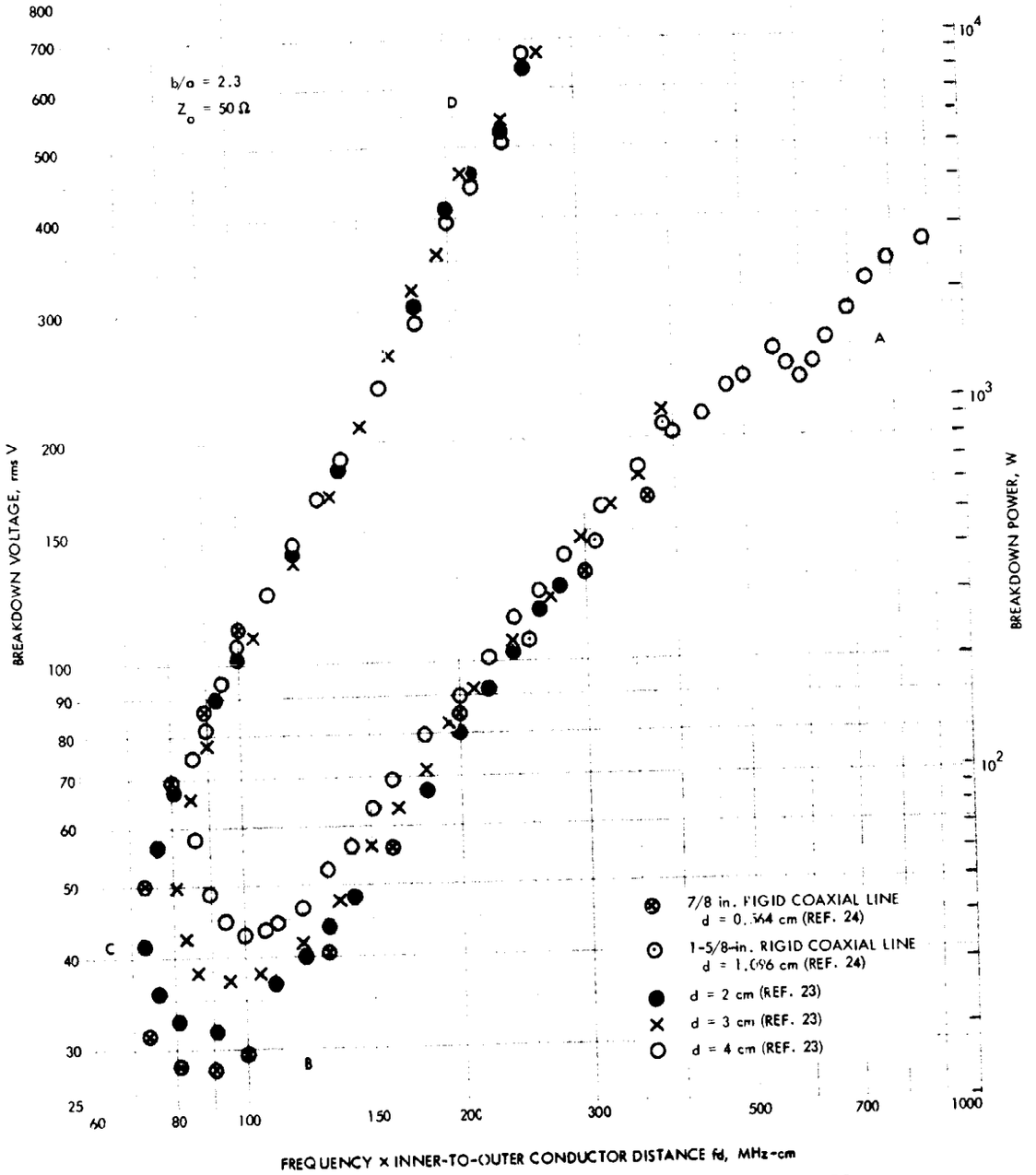

Fig. 1. Multipacting region for coaxial transmission lines, $Z_o = 50\ \Omega$

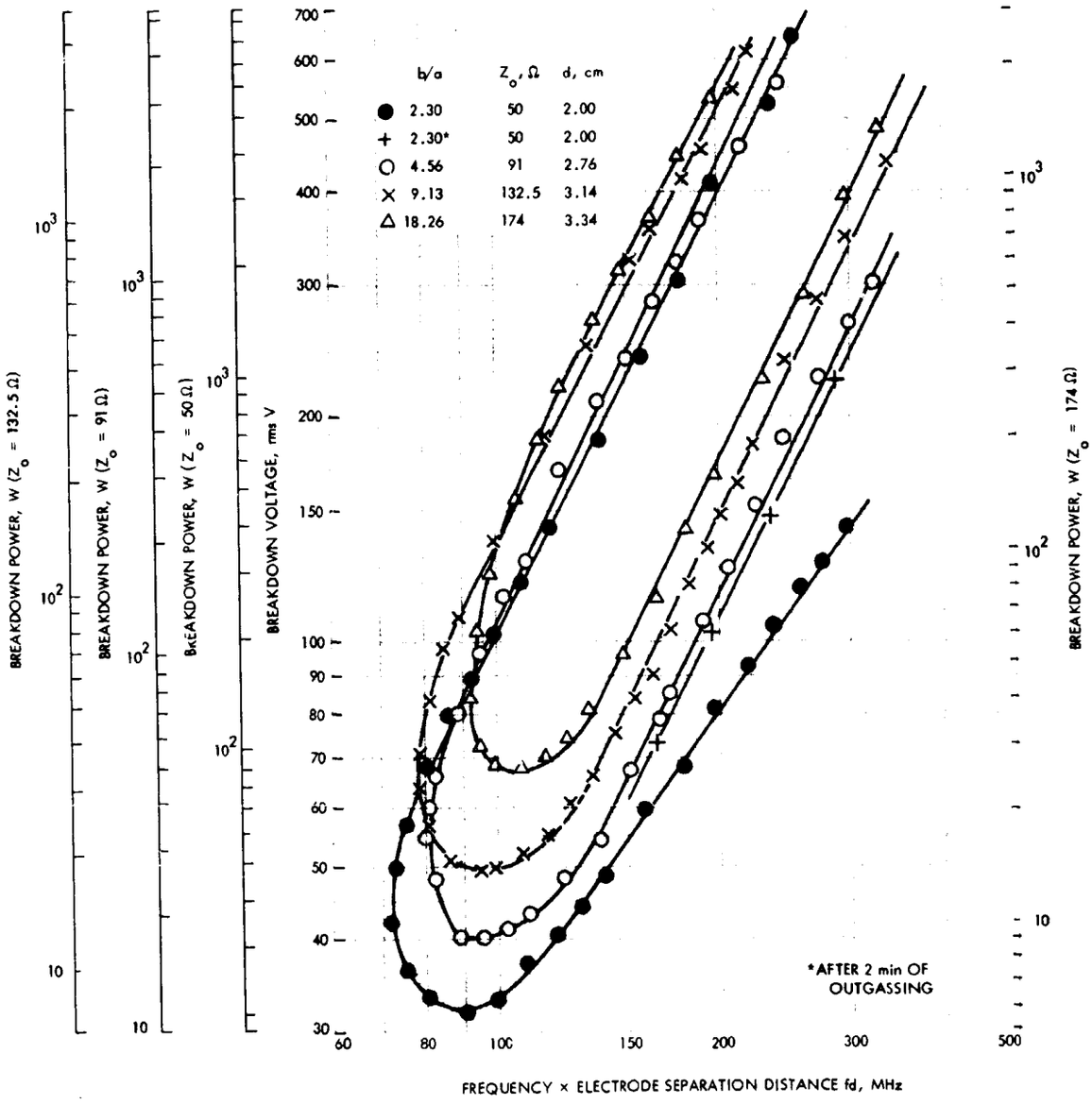

Fig. 2. Multipacting region for coaxial transmission lines with varying values of Z_o

components were used (Ref. 20), and in the frequency ranges of 150–800 and 1700–2400 MHz, where a coaxial transmission line system was employed (Ref. 24). Breakdown voltage is plotted as a function of the similarity parameter *fd*. Multipacting occurs at points within the region bounded by the data points. According to the scaling relations, these data should form one universal curve for multipacting. The experimental data confirm this fact except for the boundary *BC* which decreases slightly with decreasing *d*. A discussion of this point is provided in Refs. 20 and 24.

The presence of higher order modes is indicated by the discontinuity of *AB* for large values of *fd* (Refs. 10 and 20). The ordinate of Fig. 1 is alternately given in terms of power. It must be emphasized that this conversion is made on the basis that no mismatches are present in the line. If the line is not perfectly matched, the breakdown power levels must be derated accordingly.

To determine the multipacting breakdown levels of a given coaxial line, the following procedure is employed: from the frequency and line size, the respective *fd* value is calculated. A vertical line is then drawn for this value of *fd* in Fig. 1. This vertical line intersects the lower and upper multipacting boundaries. The lower boundary represents the minimum voltage while the upper boundary is the maximum voltage at which multipacting occurs. A qualitative explanation for this behavior can be stated. At voltages lower than the minimum and higher than the maximum, the electrons travel too slow and too fast, respectively, and cannot maintain proper phase relations with the RF field to produce multipacting. Similar arguments can be used to explain the finite range of *fd* for which multipacting occurs. Note that multipacting will not occur for values of *fd* lower than 70 MHz-cm; this represents the cutoff situation.

When using Fig. 1, one very important characteristic pertaining to the lower curve *AB* must be noted. The boundary *AB* represents the threshold conditions for multipacting. However, boundary *AB* shifts to higher voltages with the occurrence of multipacting and the consequent outgassing of the electrodes (Fig. 2). This means that if the multipacting discharge is allowed to continue for a short time, it could eventually raise the voltage required for breakdown sufficiently high to extinguish the discharge. This property has been used to advantage in linear accelerators (Ref. 17). In the case of the coaxial transmission lines, however, a brief breakdown still corresponds to an interruption in communications. Furthermore, if the transmission line is not properly vented so as to handle the outgassing load, pressure may build up inside the transmission line. If this were to happen, ionization (higher pressure) breakdown could take over and permanent damage to the line could be sustained (Ref. 5). Thus, the threshold values for multipacting should be used when designing breakdown-free lines.

D. Higher Impedance Coaxial Transmission Lines

Two factors motivated the investigation of higher-impedance coaxial transmission lines. First of all, there was a need to determine whether higher-impedance lines represented any advantage in terms of power-handling capability. Secondly, because of the increase in non-uniformity of the field configuration, higher-impedance lines offered a more rigorous test for the scaling relations.

Shown in Fig. 2 are the data for various cases of b/a and corresponding characteristic impedance Z_o. Again, the ordinate is alternately given in terms of power for each case of Z_o. It is seen that an increase in Z_o does not always result in an improvement in power handling capability. Therefore, increasing the impedance is not necessarily advantageous and Fig. 2 should be used to check each situation of interest.

According to the scaling laws, each set of data for a given value of Z_o is a universal curve for that particular value of Z_o. Figure 3 shows a check of these scaling relations for $b/a = 9.13$. As in the 50 Ω coaxial line, the correspondence is very good except for the boundary *BC* which again decreases with decreasing *d*.

E. Magnetic Fields and DC

When magnetic fields are present, scaling laws can be derived (Ref. 22). Experimental studies of multipacting in a magnetic field have been very limited (Ref. 22). Consequently, these scaling relations have not been verified.

The simultaneous application of dc and RF voltages to the coaxial electrodes is of interest since the dc bias serves as a potential means of eliminating or preventing multipacting. Scaling relations have been derived and experimentally verified for such configurations; Refs. 20 and 22 provide detailed explanations. A typical set of experimental data is shown in Fig. 4. The reason for presenting these data is to indicate that although a dc bias can be used to prevent multipacting it would have to be fairly high. In many cases, therefore, this method would be undesirable.

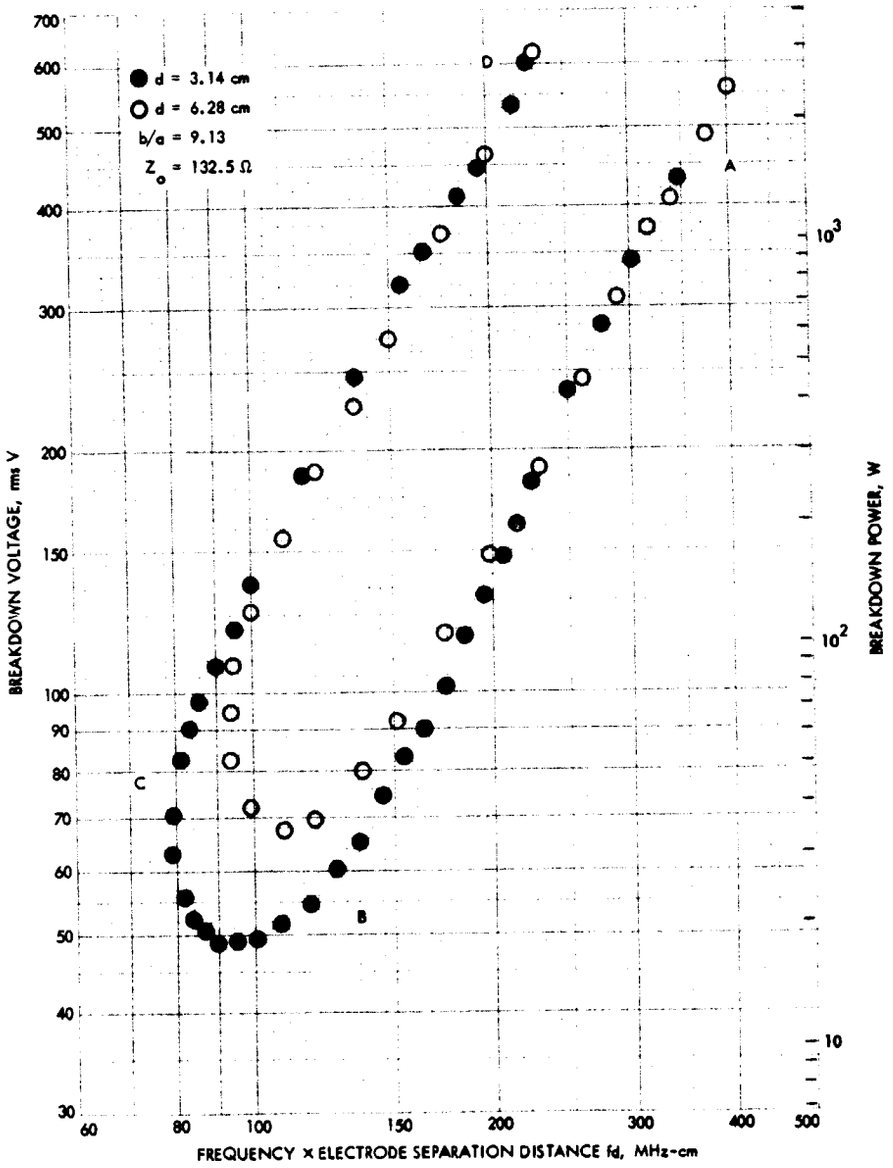

Fig. 3. Multipacting region for coaxial transmission lines, Z_o = 132.5 Ω

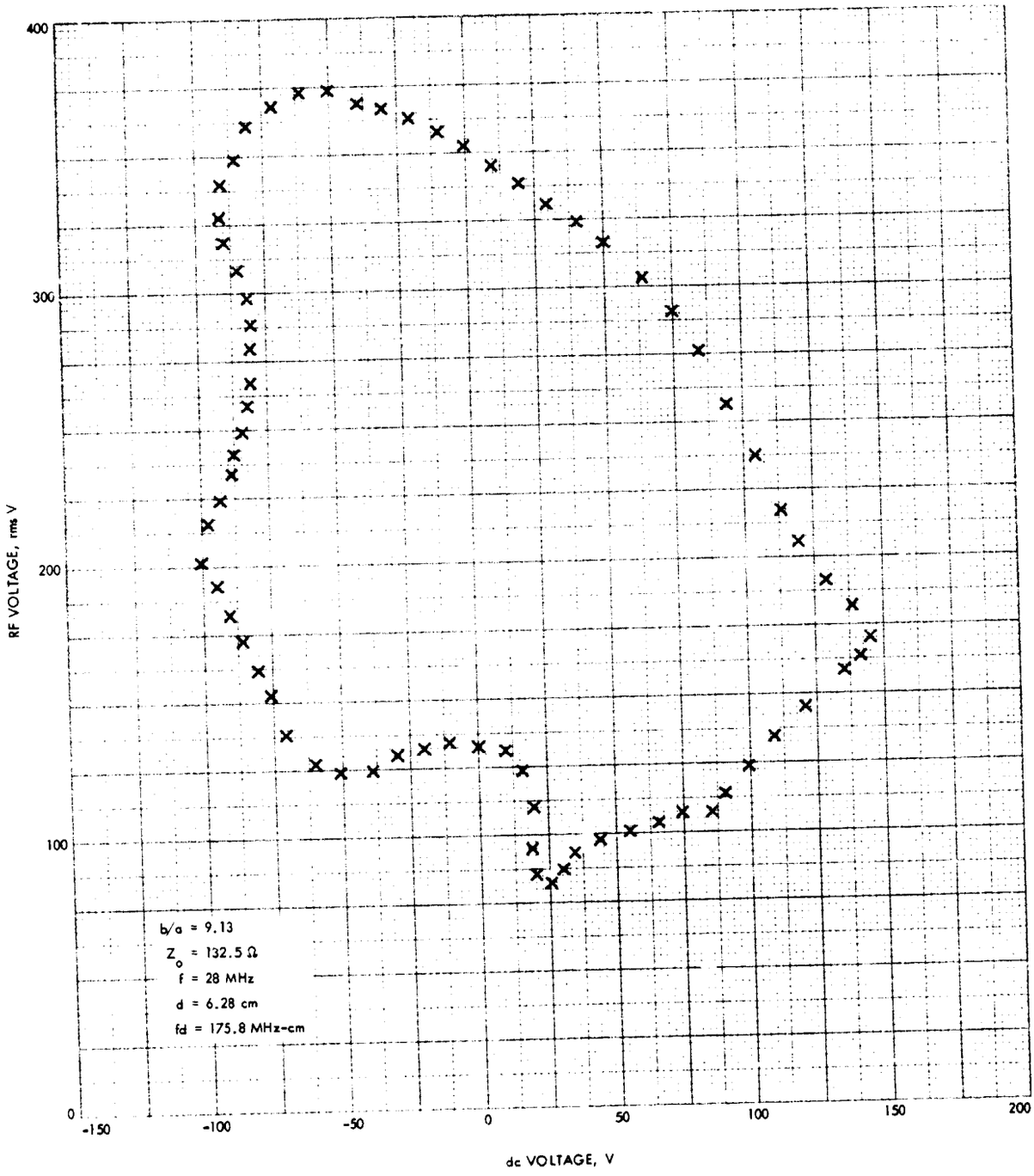

Fig. 4. Multipacting in the presence of a dc voltage

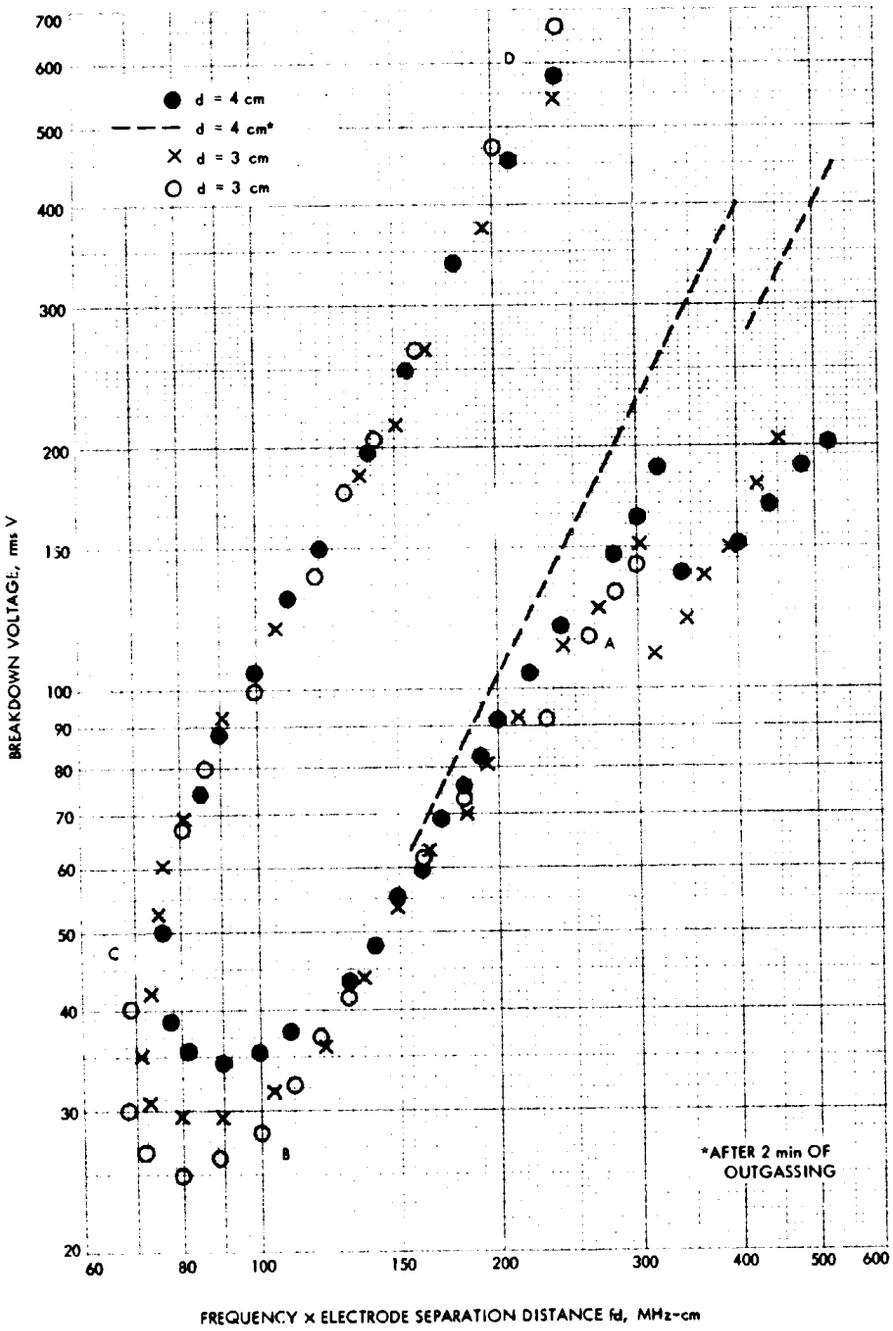

Fig. 5. Multipacting region for parallel electrodes

F. Uniform Fields

Multipacting data were also obtained for the parallel plates geometry and are shown in Fig. 5. In this case, d represents the separation distance between the parallel plates. The availability of higher RF voltages resulted in additional data points than were previously available (Ref. 10). The data in Fig. 5 are very similar to those in Fig. 1. This is to be expected since the fields for 50 Ω coaxial transmission lines are not significantly different from uniform fields. The electron trajectories are also similar. This fact was demonstrated in a computer study of the electron trajectories (Ref. 25); it should be mentioned that in this computer study, the scaling laws were utilized. As a result, only a small number of solutions were needed to cover the entire breakdown region.

IV. Ionization Breakdown

Ionization breakdown occurs at pressures higher than those for multipacting. This high-pressure RF breakdown must be considered for two types of missions. One type is where there is a requirement to turn on the high-power RF prior to launch and leave it on during ascent through the earth's atmosphere. *Mariners VI* and *VII* had this power turnon requirement. Some voltage breakdown problems were encountered in these missions and are discussed in Section IV-D. Another type of mission is the lander mission involving a planet whose surface pressure is in the pressure range of ionization breakdown. An example of this is the *Viking* project which will place a lander on the surface of Mars. The pressure on the surface of Mars is several torr. For missions involving hard-vacuum pressures, ionization breakdown could still occur if the transmission line is not properly vented or if significant outgassing exists in the breakdown region.

Ionization breakdown is considerably more complex than multipacting. In ionization breakdown, electrons are produced through collisions between electrons and gas molecules. Therefore, ionization breakdown is dependent not only on pressure but on the type of gas as well. Depending on the range of the experimental parameters, different breakdown mechanisms are involved. Studies have been made of ionization breakdown in the coaxial line geometry, but these have generally been restricted in terms of experimental parameters and breakdown processes (Refs. 12, 26, and 27). Moreover, these breakdown data have been displayed in complex schemes difficult to apply in practice. The motivation for the studies on ionization breakdown in coaxial lines was, therefore, twofold. First, there was a lack of experimental data covering a wide range of experimental parameters. Second, there was a need to display these data in a scheme that would be practical and easily applied by a design engineer.

A. Coaxial 50-Ω Transmission Lines

The experimental data obtained for the 50-Ω coaxial transmission line (Ref. 28) is summarized in Fig. 6. Here, p is pressure and, as before, f and d are frequency and inner-to-outer conductor distance, respectively. It must be emphasized that ionization breakdown is dependent on the type of gas and that the ionization breakdown data in Fig. 6 are for air only. Brown and MacDonald (Ref. 29) showed that similarity parameters for RF voltage breakdown can be determined from dimensional analysis. The similarity parameters in Fig. 6 are, however, different from those used by Brown and MacDonald and have been selected for practical reasons. If one is interested in the breakdown behavior of a given coaxial line operating at a particular frequency, he merely computes the corresponding fd. By referring to Fig. 6, he not only has breakdown power as a function of pressure, but also information on the effects of changing either frequency or line size.

The fd-p/f plane shown in Fig. 7 is very helpful in identifying the breakdown processes involved in the data contained in Fig. 6. The limits are similar to those discussed by Brown and MacDonald (Ref. 29). Although they are in the form of lines, they are meant to indicate transition rather than abrupt change. The mean free path limit represents the condition that the electron mean free path is equal to d. The mean free path limit, therefore, separates the ionization and multipacting breakdown regions. Multipacting occurs when p/f is less than this limit while ionization breakdown occurs when p/f is greater. Thus, Fig. 6 includes multipacting as well as ionization breakdown data.

As discussed in Section III-C, multipacting will not exist for fd lower than 70 MHz-cm. The multipacting cut-off limit indicates this cutoff condition. It should be pointed out that the multipacting data in Fig. 6 corresponds to the lower boundary of Fig. 1. The upper boundary, above which multipacting will not occur, is not shown in Fig. 6. Notice that, as discussed earlier, the multipacting data in Fig. 6 are independent of pressure.

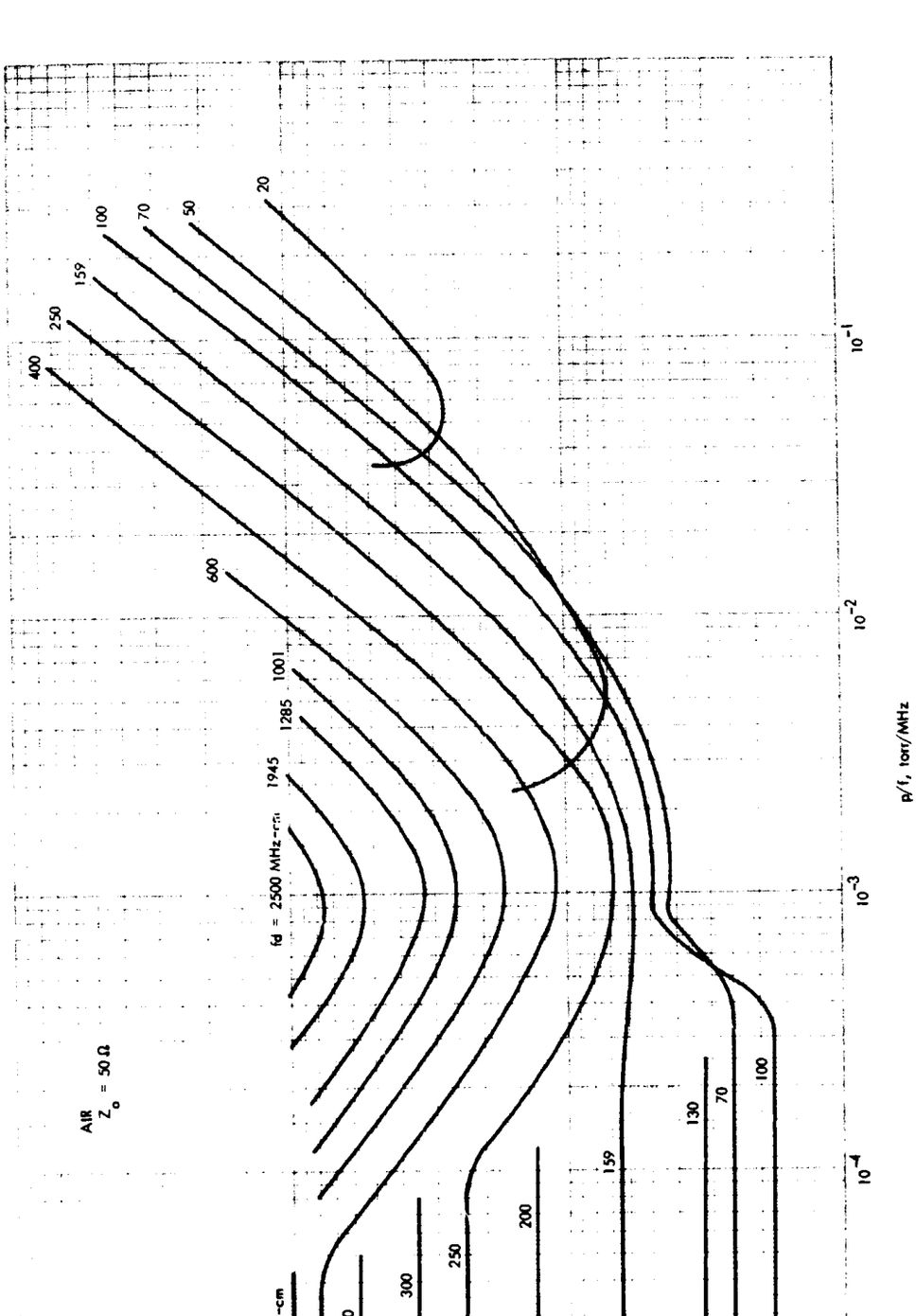

Fig. 6. RF voltage breakdown in coaxial transmission lines, $Z_0 = 50\ \Omega$

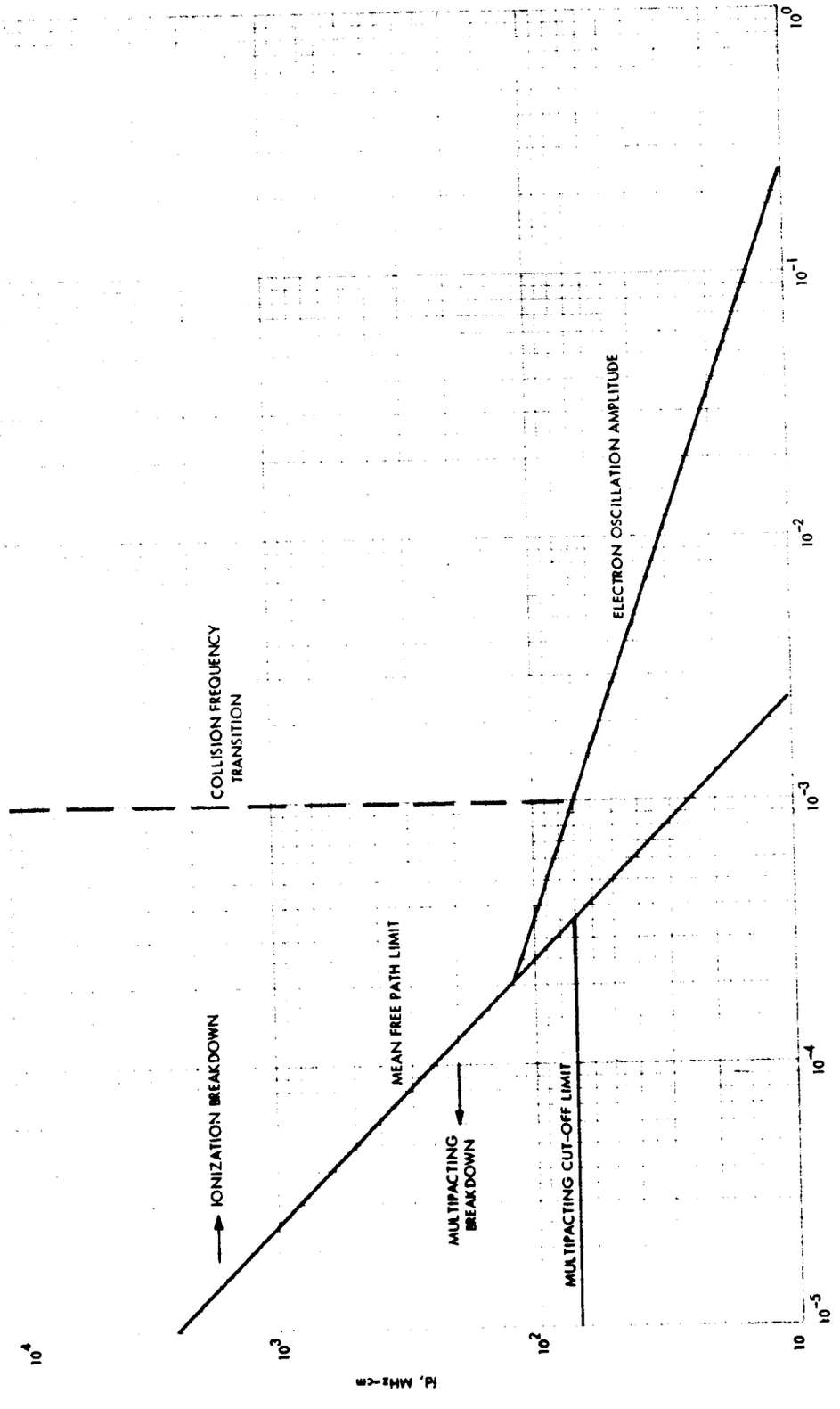

Fig. 7. The fd-p/f plane showing limits of breakdown processes

When discussing ionization breakdown, it is convenient to use the two ranges of fd presented below.

1. The $fd > 100$ MHz-cm range. Under these conditions, frequency is sufficiently high and the inner-to-outer conductor distance sufficiently long that the electrons are not swept out of the discharge region by the field as, for instance, in the case of dc breakdown. Instead, the electrons are concentrated in the center of the discharge region and slowly diffuse away towards the conductors. The speeds are so low that the electrons produce essentially no secondary effects at the electrode surfaces. Breakdown of this type is termed diffusion-controlled or microwave breakdown (Refs. 11–13).

The minima of the diffusion-controlled curves occur at approximately $p/f = 10^{-3}$ torr/MHz. This is equivalent to saying that each minimum occurs at a pressure given in microns (1 micron = 10^{-3} torr) equal to the frequency given in MHz. For example, the minimum for the frequency 2000 MHz occurs at 2000 microns or 2 torr. The $p/f = 10^{-3}$ torr/MHz line is called the collision-frequency transition. At the collision-frequency transition the applied frequency and the electron-molecule collision frequency are approximately equal, and energy transfer to the electrons from the field is at a maximum. If pressure is increased, the electron-molecule collision frequency increases, the energy gained by electrons from the field per mean free path decreases and the breakdown level

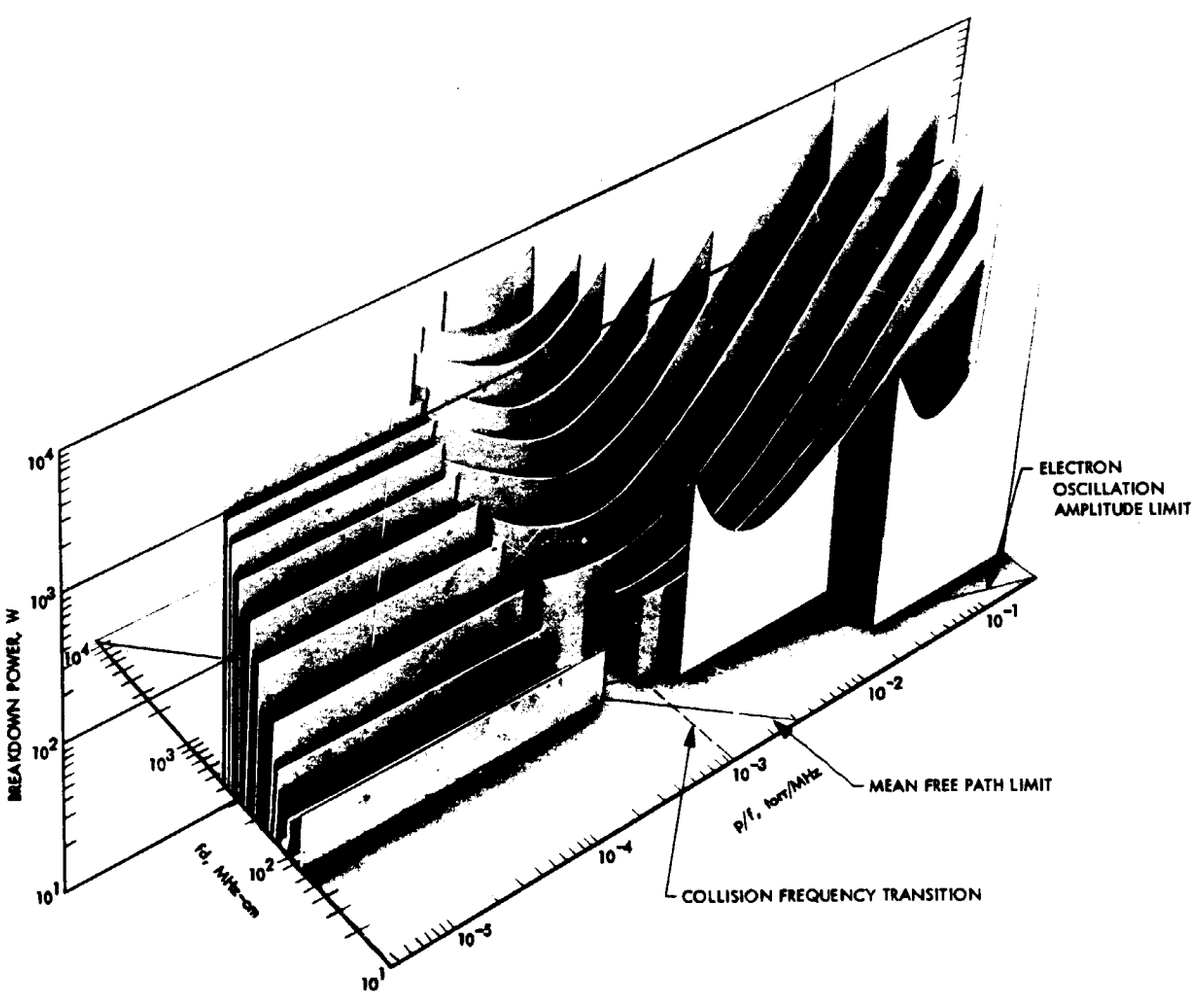

Fig. 8. Three-dimensional surface representing RF breakdown in 50-Ω coaxial transmission lines

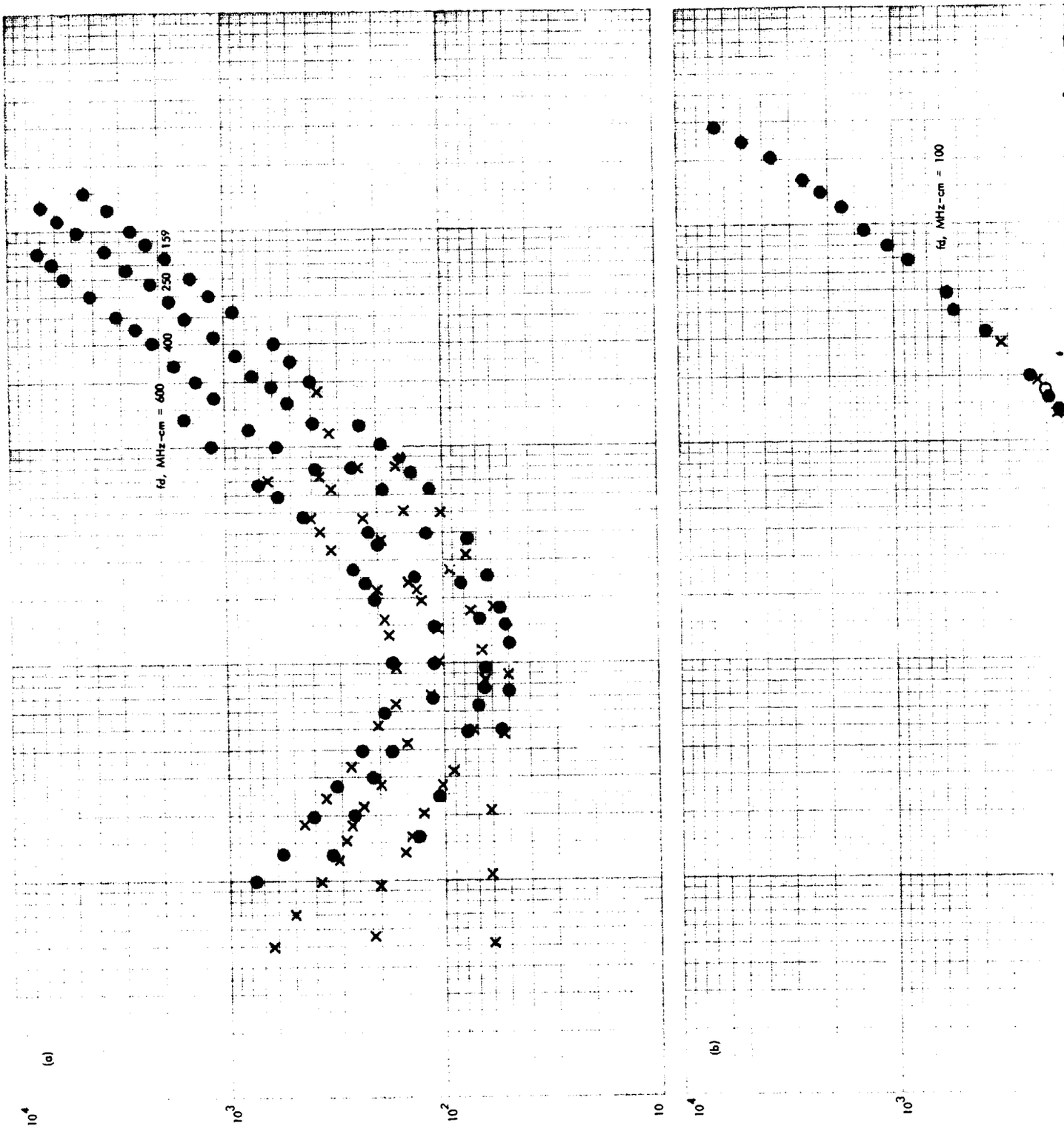

FOLDOUT FRAME 1

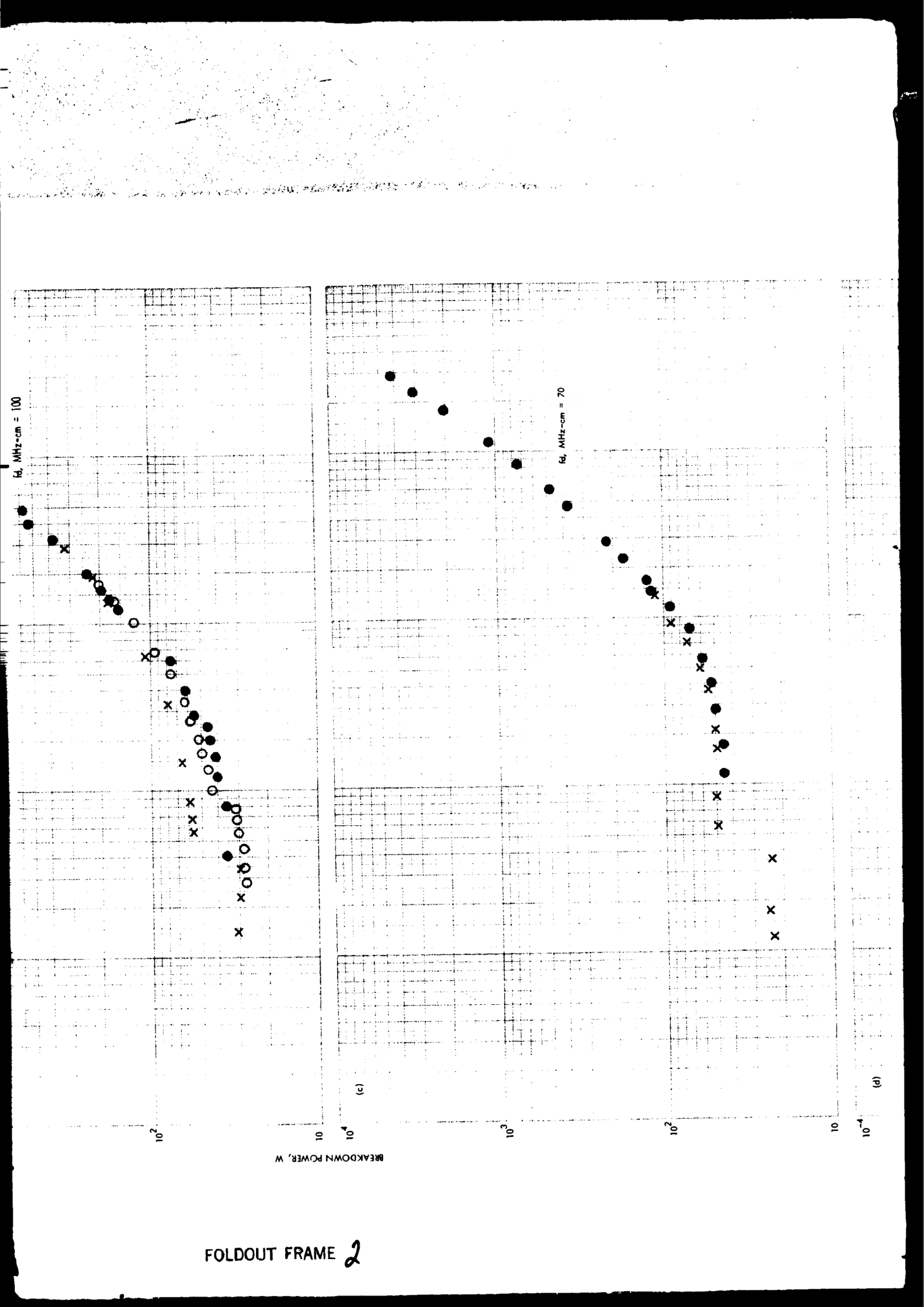

FOLDOUT FRAME 2

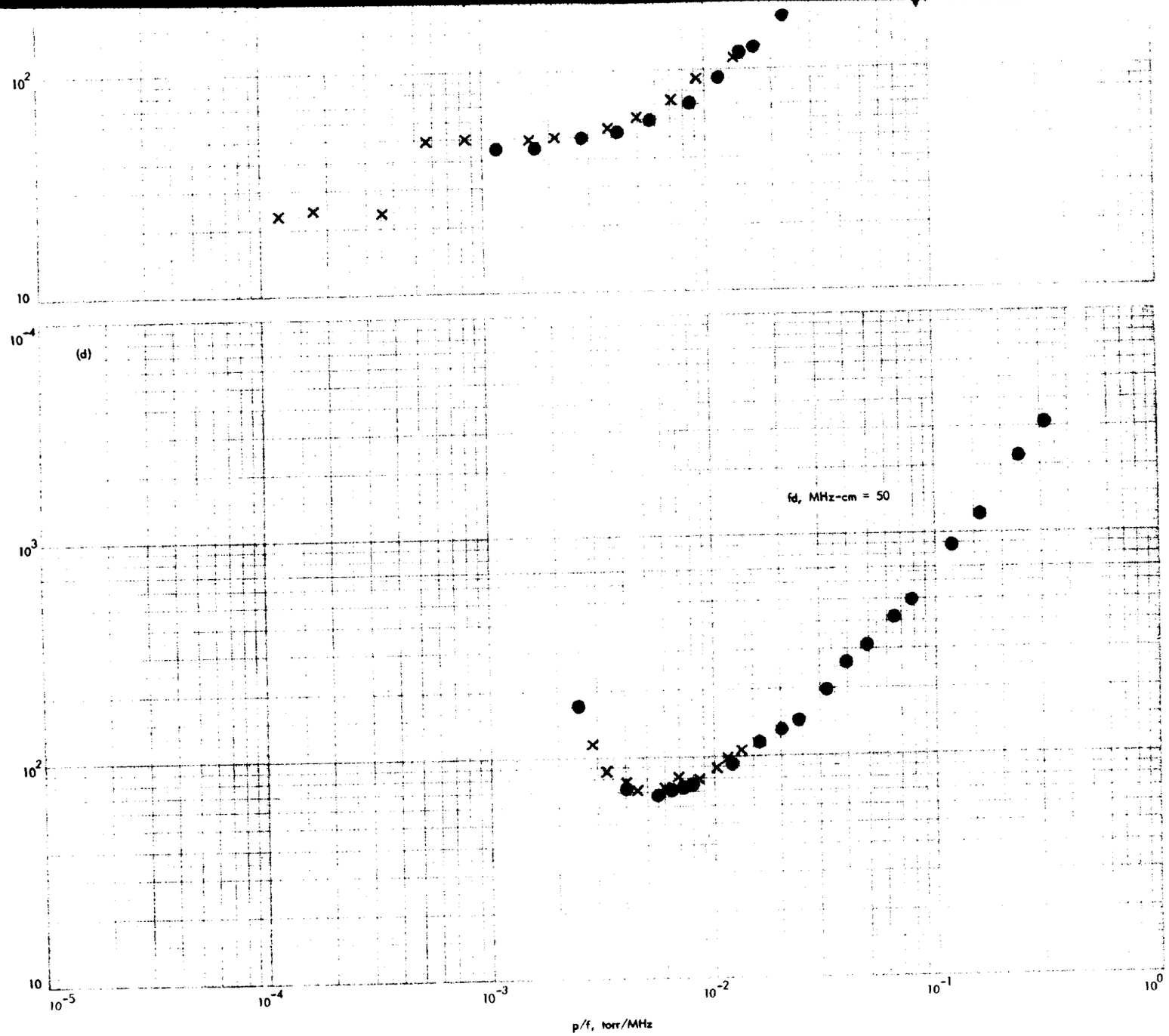

Fig. 9. Typical RF breakdown data obtained for 50-Ω coaxial transmission lines

FOLDOUT FRAME 3

increases correspondingly. In a perfect vacuum, the electrons oscillate with their velocity 90 deg out of phase with the RF field and no energy is gained by the electrons from the field. The electrons gain energy from the field only by undergoing collisions with the gas molecules. A decrease in pressure from the collision frequency transition corresponds to an increase in loss of energy transfer from the field to the electrons. Breakdown power, therefore, rises with decreasing pressure.

2. The fd < 100 MHz-cm range. When the applied frequency is sufficiently low or the d is sufficiently short, the amplitude of oscillation of the electron cloud approaches d and the inner and outer conductors enter the breakdown picture. This situation occurs when fd is less than 100 MHz-cm. Under such conditions, the loss of electrons is governed by mobility; Brown (Ref. 11) has termed this type of breakdown mobility-controlled breakdown. It must be emphasized that the transition from diffusion-controlled to mobility-controlled breakdown is gradual and occurs at approximately 100 MHz-cm. The oscillation-amplitude limit corresponds to the condition for which the amplitude of oscillation of the electron cloud is equal to d. At this limit, electrons are lost to the inner and outer conductors and the power required for breakdown rises rapidly. This behavior is illustrated in the data for fd equal to 50 and 20 MHz-cm in Fig. 6. As an aid in visualizing the universal curves in Fig. 6, a three-dimensional surface representing breakdown may be constructed by combining Figs. 6 and 7. The resulting three-dimensional representation is shown in Fig. 8.

Shown in Fig. 9 are typical experimental data used to construct Fig. 6. For each value of fd there are two sets of data taken at two frequencies. These two frequencies differ by as much as seven to one, and it is seen that the scaling correspondence is remarkably good. There is a spread in the results for fd = 100 MHz-cm at the lower values of p/f. This is not surprising since this is a region of several transitions and breakdown is somewhat dependent on surface conditions.

The minimum power handling capability is of particular interest. Shown in Fig. 10 is the minima for ionization breakdown as a function of fd for $fd > 100$ MHz. The multipacting data are also included for comparison.

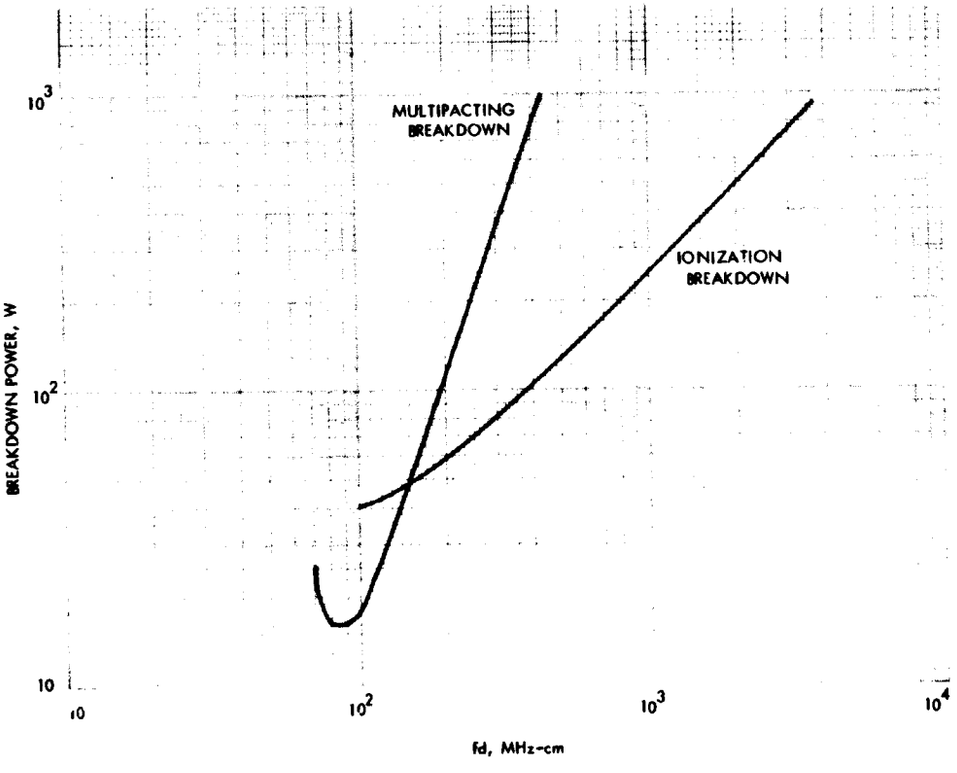

Fig. 10. Minimum power handling capability in terms of fd, Z_0 = 50 Ω

When fd is less than 145 MHz-cm, the ionization breakdown power level is higher than the multipacting power level whereas the reverse is true when fd is greater than 145 MHz-cm.

The scheme used in Fig. 6 to depict breakdown data for the 50-Ω coaxial line may be used for higher impedance coaxial lines. It may also be used to represent breakdown in gases other than air. The results of these cases are given in the following sections.

B. Higher Impedance Coaxial Transmission Lines

Shown in Figs. 11 and 12 are the universal curves obtained for two cases of Z_o higher than 50 Ω: 74 and 91 Ω. As would be expected, the curves are similar to those for the 50-Ω line. The multipacting-to-ionization transition as well as the oscillation amplitude limit characteristics are evident in the data. The multipacting results were discussed in Section III-D and will not be repeated here.

For convenience of comparison, the minimum power handling figures for ionization breakdown are listed in Table 1. As can be seen, the minimum breakdown voltage increases as the characteristic impedance is increased for a given value of fd. This can be explained by the fact that as b/a is increased, the fields become more non-uniform so that electron loss by diffusion out of the breakdown area is also higher. In order to make up for this loss, the voltage must be increased. Even though breakdown voltage increases with impedance, it is important to note that this does not always result in an increase in breakdown power. There is appreciable improvement in power handling capability for smaller values of fd; e.g., fd = 55 MHz-cm. These smaller values of fd are in the oscillation amplitude limit region. An increase in electron diffusion loss due to the non-uniformity of the fields may be regarded as equivalent to a shortening of d. Since along the oscillation amplitude limit there is a rise in breakdown power as fd decreases (Fig. 6), improvement in power handling capability for higher impedances would be expected. Unfortunately, for S-band frequencies, fd is generally greater than 100 MHz-cm. For these cases, there is little, if any, improvement in higher impedances. It can therefore be concluded that for most cases, a higher characteristic impedance coaxial transmission line offers no significant advantages in terms of ionization breakdown.

Table 1. Minimum breakdown voltage and power for ionization breakdown for varying Z_o

fd, MHz-cm	Z_o, Ω	Breakdown voltage, V	Breakdown power, W
400	50	72.8	106
400	74	80	86.5
400	91	98	105.3
200	50	53.5	58
200	74	66.6	60
200	91	72.6	58
100	50	49	48
100	74	57.6	45
100	91	73.9	60
55	50	57.5	66
55	74	81.5	91.5
55	91	90	92

It is interesting to compare the breakdown data obtained for the 50-Ω case with that obtained for higher impedances over the entire range of p/f. These data are shown in Figs. 13–15. It is seen that there is a crossover point in each case. For pressures greater than the crossover point, less power is required for breakdown in the higher impedance case. The reverse is true for pressures less than the crossover point. This behavior can be simply explained in terms of the breakdown mechanisms involved.

Above the crossover point, pressure is high enough that breakdown activity is confined to the region around the center conductor. This is confirmed visually by the extent of the breakdown glow in the experiments conducted. For this case then, breakdown is dependent on the magnitude of the electric field in the area of the center conductor. Since this field increases with increasing impedance, breakdown occurs more easily in the higher impedance cases. For pressures lower than the crossover point, breakdown spreads to the outer conductor. Under these circumstances, an increase in the non-uniformity of the fields results in an increase in electron loss due to diffusion to the conductor walls. In order to overcome this loss, breakdown power increases. Therefore, breakdown power is higher for higher impedances. These facts are important if the transmission line must operate in a specific pressure range. Depending on the pressure range, a higher impedance may or may not be beneficial.

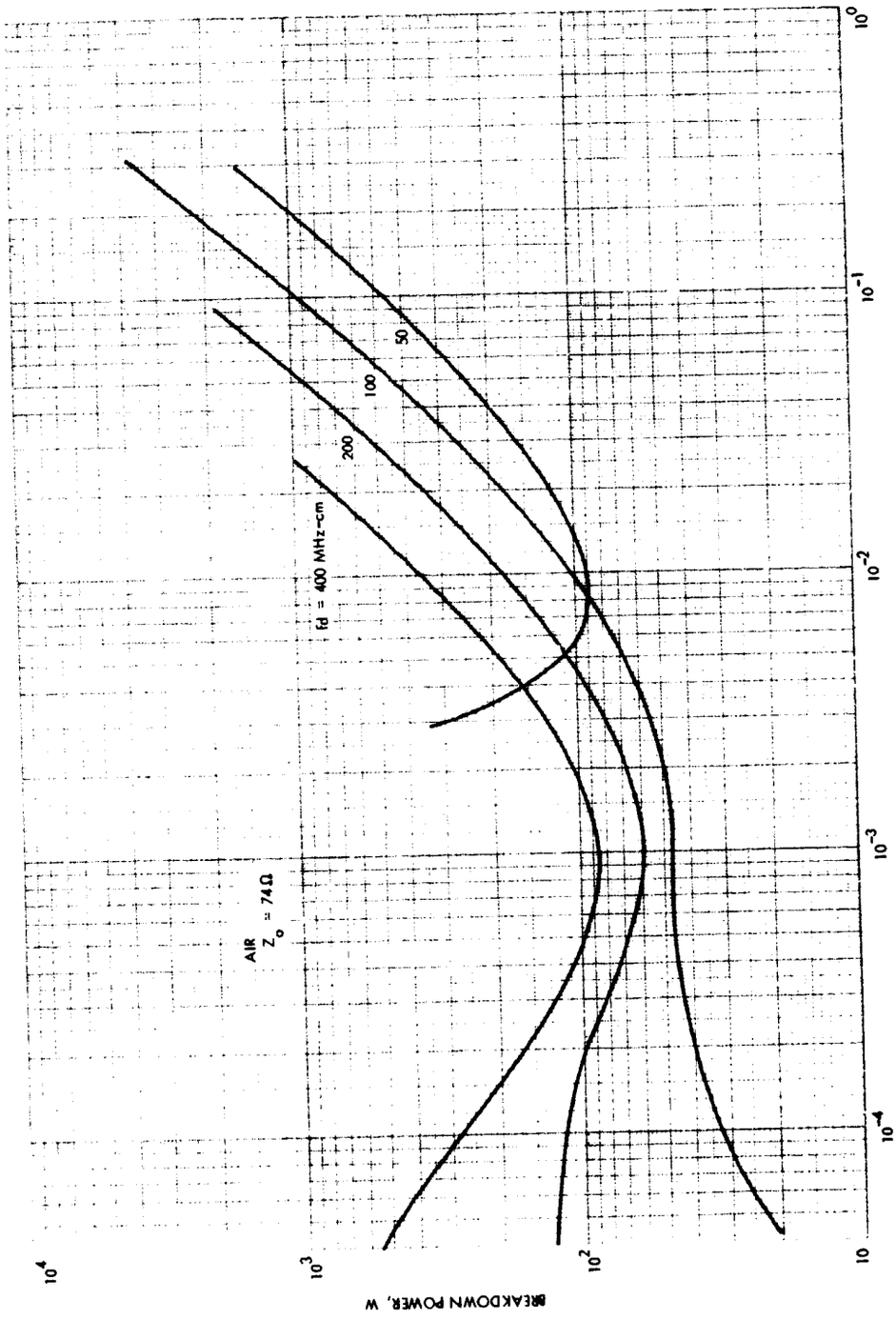

Fig. 11. RF voltage breakdown in coaxial transmission lines, Z_o = 74 Ω

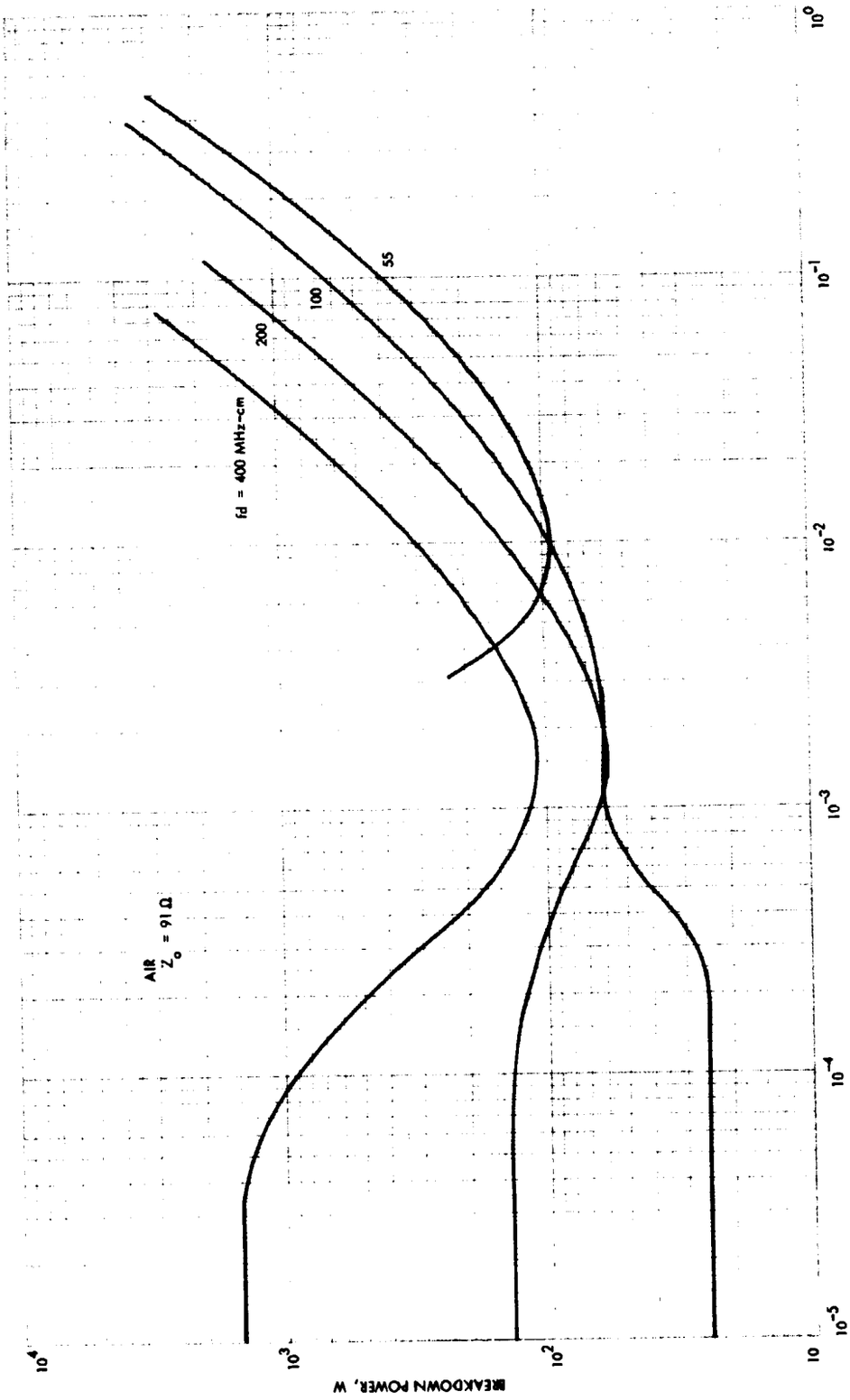

Fig. 12. RF voltage breakdown in coaxial transmission lines, $Z_o = 91\ \Omega$

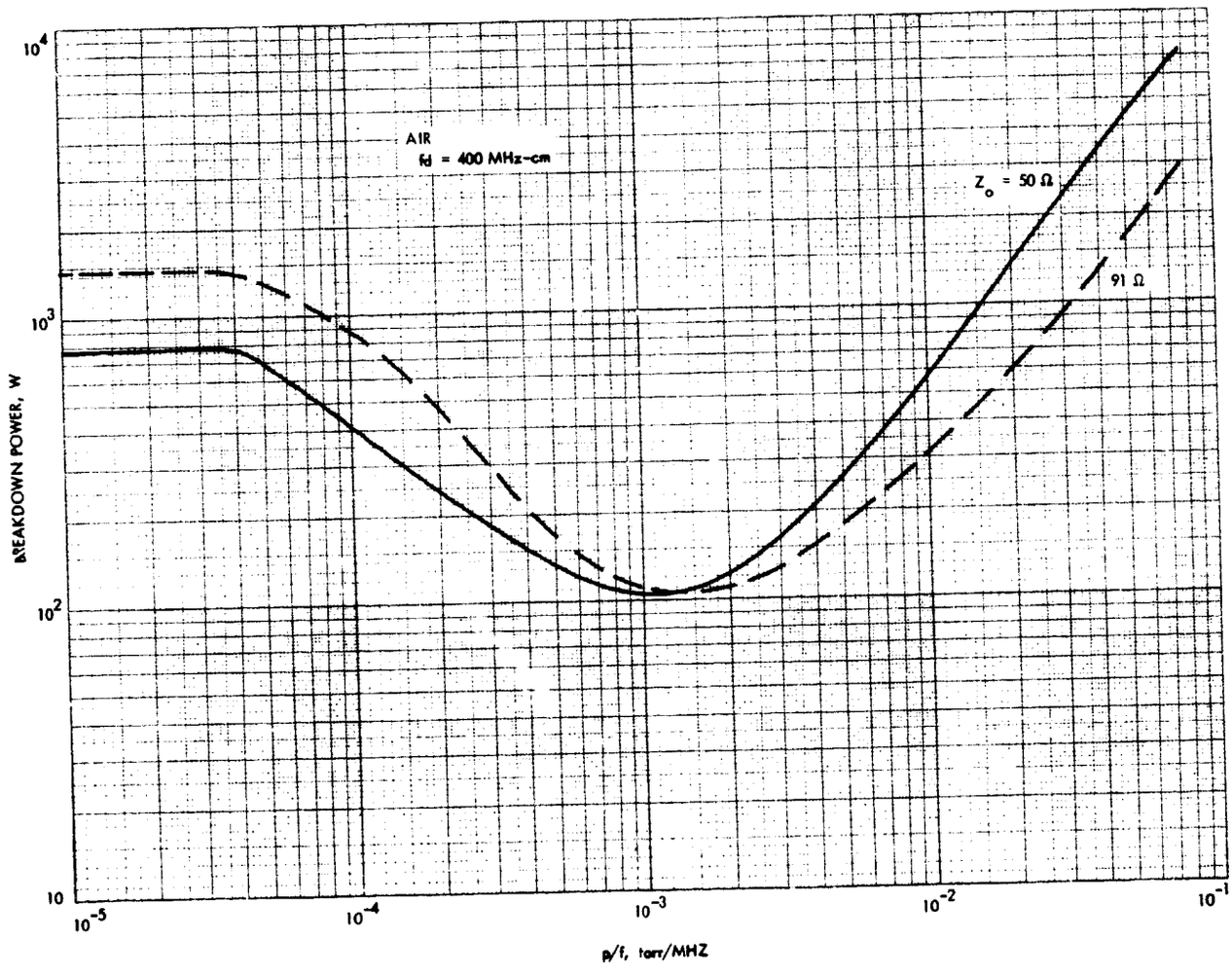

Fig. 13. Breakdown power vs p/f for fd = 400 MHz-cm, Z_o = 50 and 91 Ω

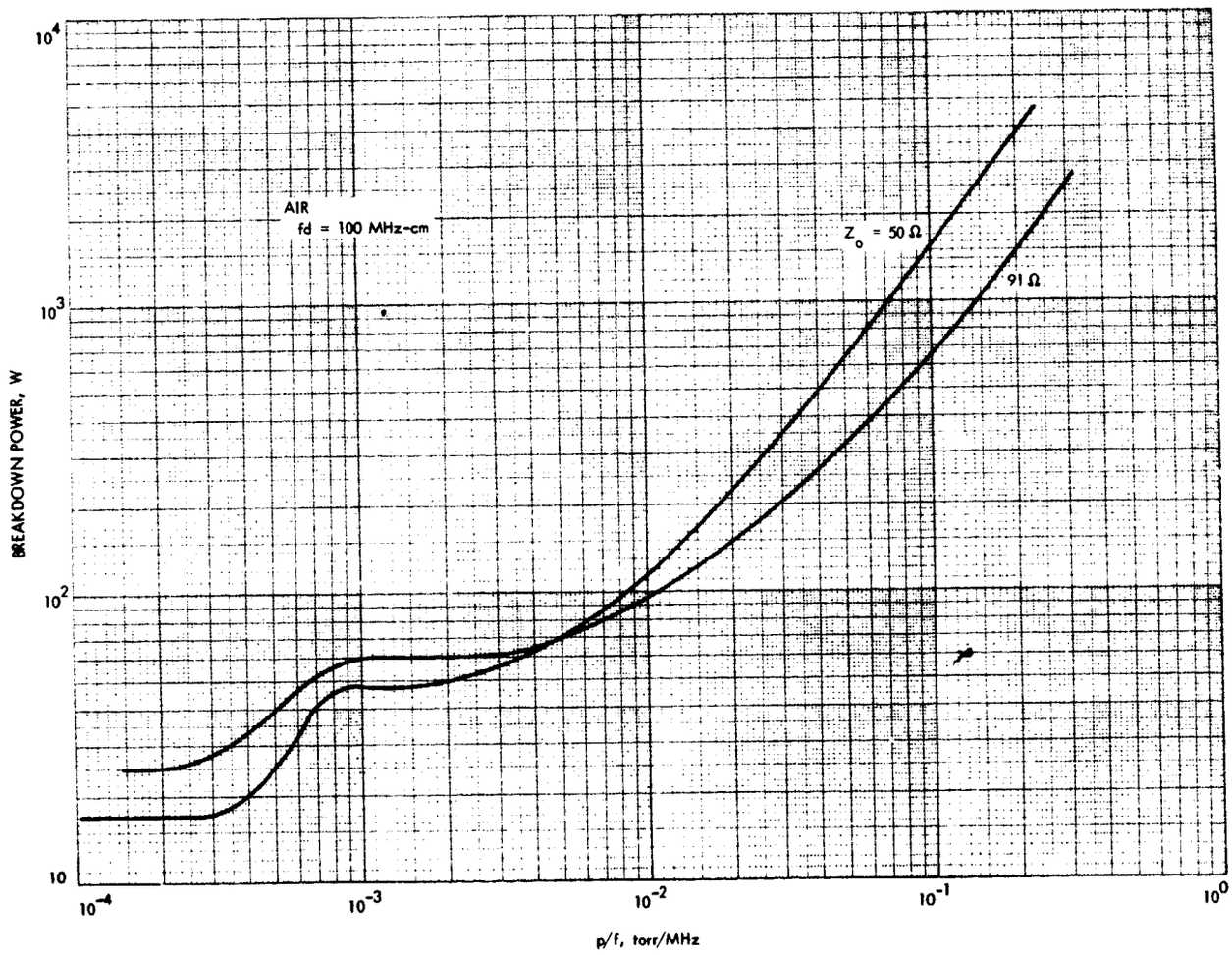

Fig. 14. Breakdown power vs *p/f* for *fd* = 100 MHz-cm, Z_o = 50 and 91 Ω

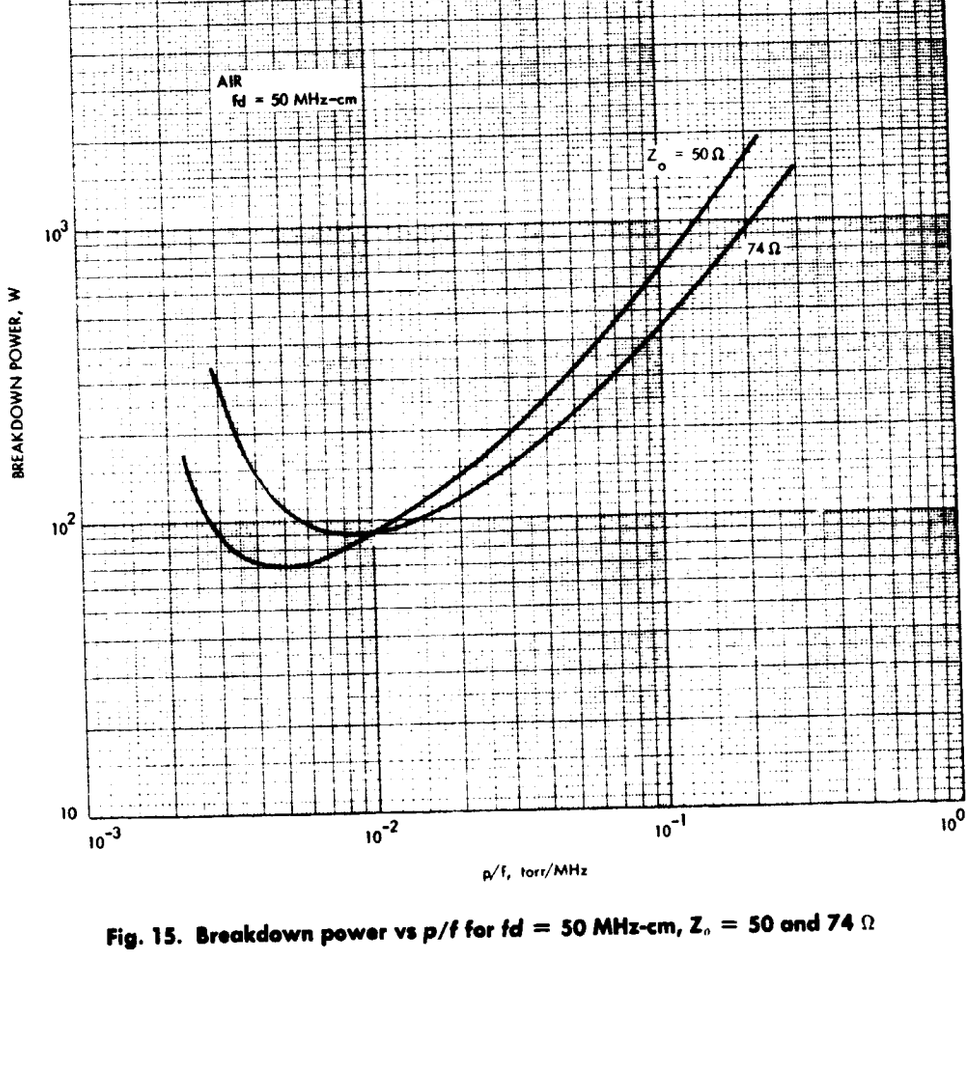

Fig. 15. Breakdown power vs *p/f* for *fd* = 50 MHz-cm, Z_o = 50 and 74 Ω

C. Gases Other than Air

As indicated previously, ionization breakdown is dependent on type of gas. Breakdown in gases such as carbon dioxide and argon are of special interest since these gases are present in planetary atmospheres; e.g., Mars. As in the case of air, there have been investigations of RF breakdown in argon (Refs. 13 and 30) but these have been restricted in range of experimental parameters. No RF breakdown data for carbon dioxide appear available for the coaxial line geometry.

The experimental setups used were similar to those used in the experiments for air (Ref. 28). The carbon dioxide and argon gases had a purity level of 99.99%. The vacuum system was evacuated to a pressure level less than 10^{-5} torr before the carbon dioxide or argon gas was admitted. Each breakdown was conducted with a fresh sample of gas. In order to measure pressure, a Granville-Phillips capacitance manometer was used. The capacitance manometer was calibrated and periodically checked against a McLeod gauge.

The data for carbon dioxide are shown in Fig. 16 while argon data are shown in Fig. 17. Breakdown levels for mixtures of argon and carbon dioxide lie between the curves for 100% argon and 100% carbon dioxide. Shown in Fig. 18 is the minimum power handling capability as a function of fd ($fd > 100$ MHz-cm) for air, argon, and carbon dioxide. As can be seen, breakdown in carbon dioxide is 12–18% lower than that of air while breakdown in argon is 45–60% lower. It should be pointed out that the expected concentration of argon in the

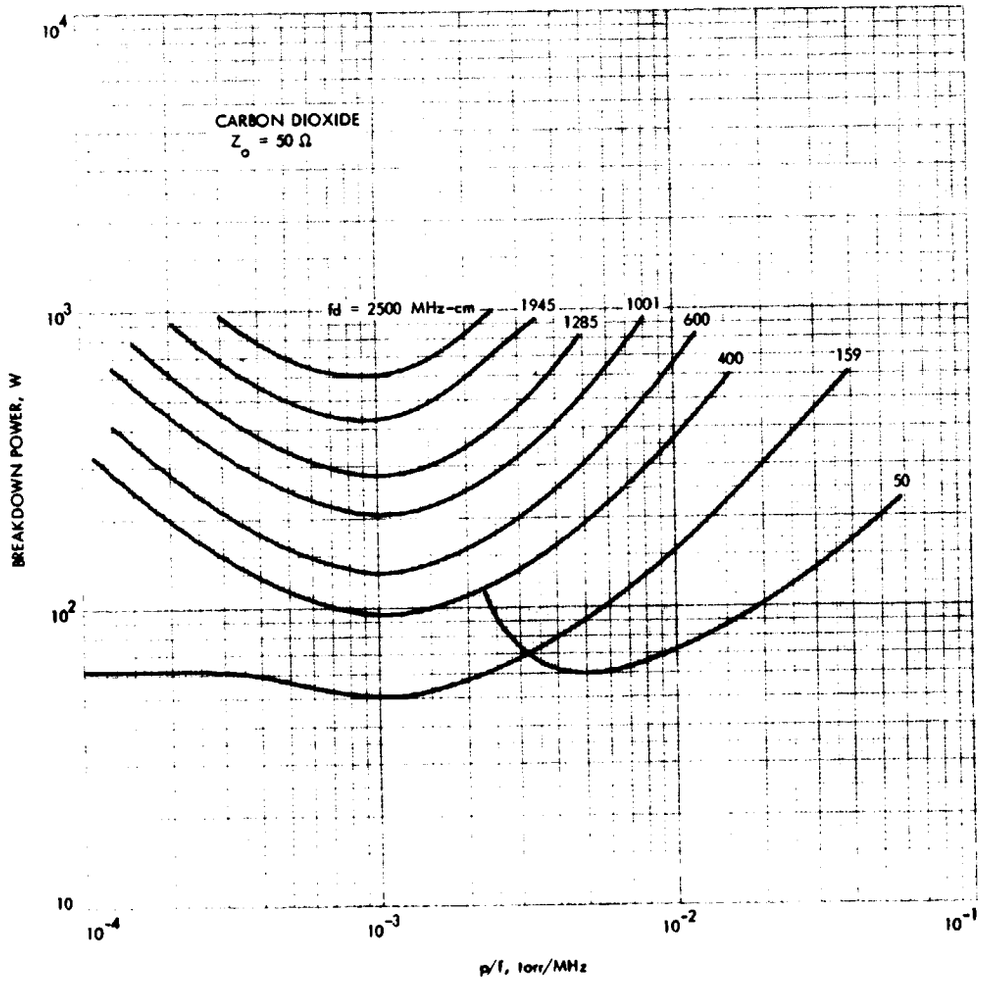

Fig. 16. Breakdown in carbon dioxide, Z_o = 50 Ω

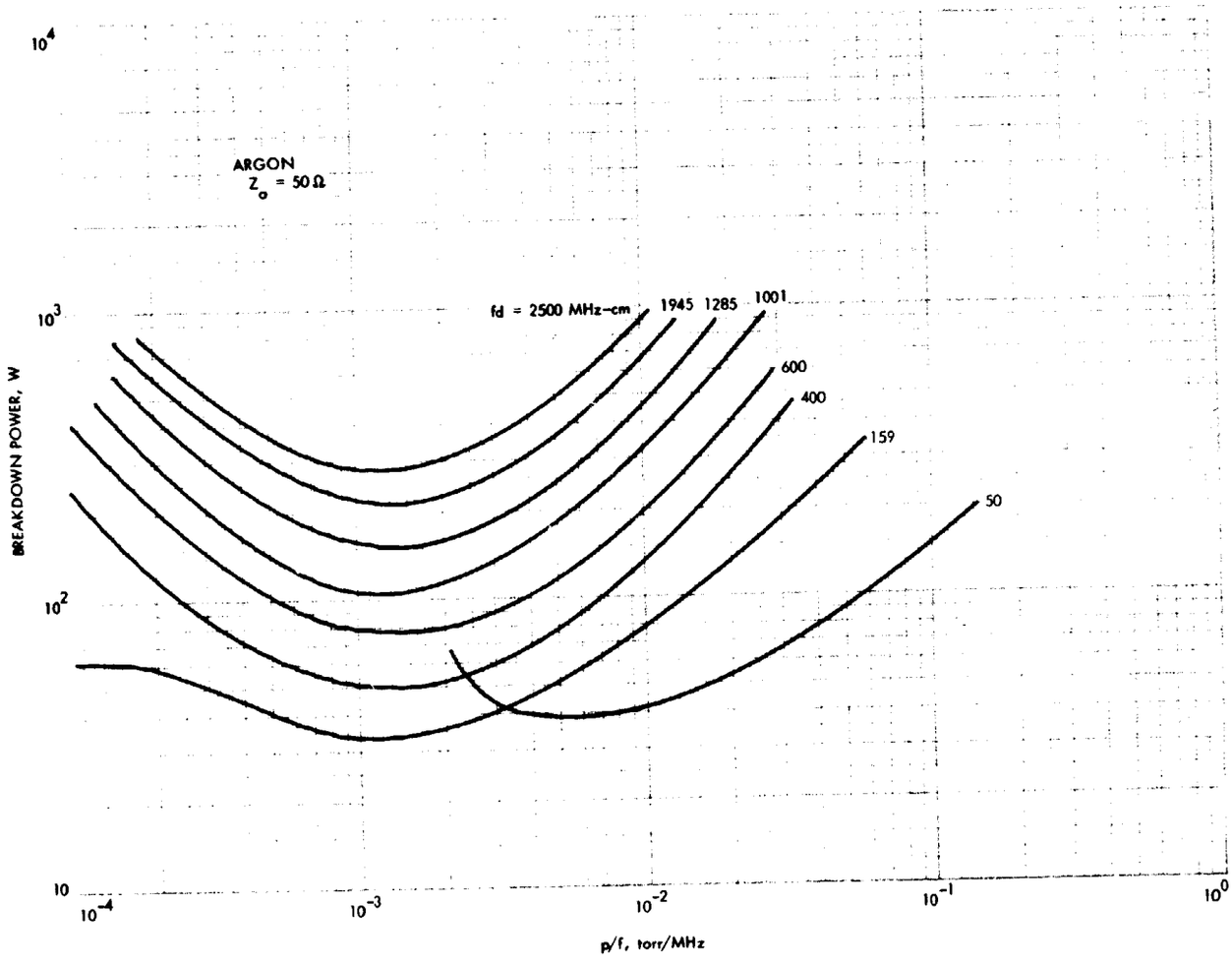

Fig. 17. Breakdown in argon, $Z_o = 50\ \Omega$

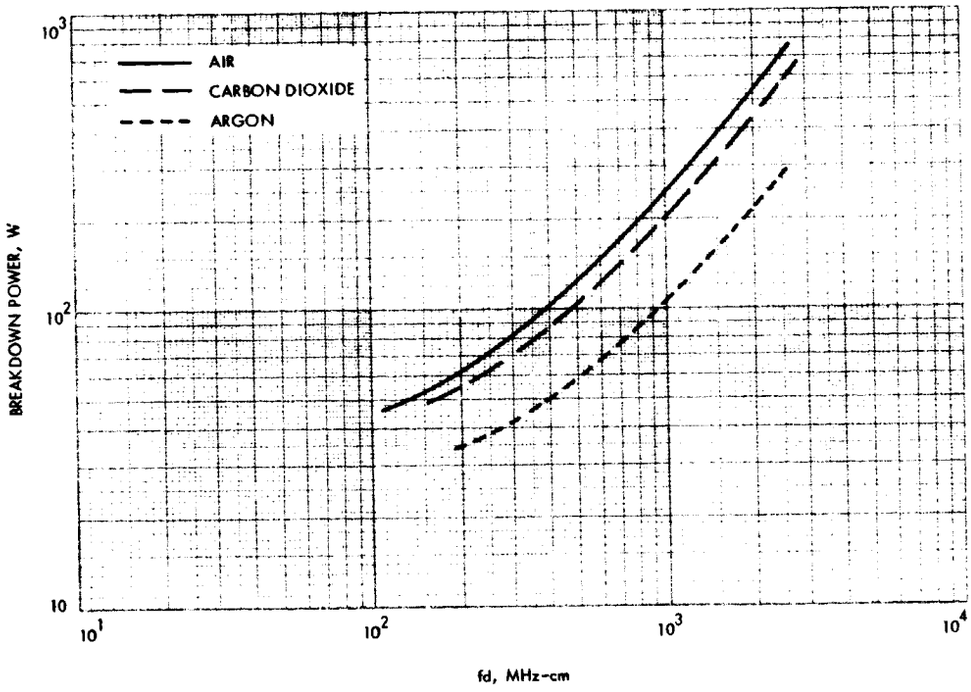

Fig. 18. Minimum power handling capability in terms of *fd* for air, carbon dioxide, and argon

Martian atmosphere is small so that the 100% argon data should only be regarded as extreme values. Figs. 16 and 17 are for $Z_o = 50\ \Omega$. Experiments were also run for $Z_o = 91\ \Omega$ and the results are shown in Figs. 19 and 20.

D. Uniform Fields

Many studies have been made of ionization breakdown in uniform fields in air (Refs. 11–13). Some nomographs (Refs. 27 and 31) exist, but these cover limited experimental ranges and a complex computation procedure must be used. The scheme used in Fig. 6 may also be used for the uniform fields data.

The results for the uniform field geometry are shown in Fig. 21. Both multipacting and ionization breakdown data are included. For the uniform fields geometry, d represents the gap distance. The solid curves represent data obtained experimentally while the dotted curves extrapolated data. For the fd range of 20–250 MHz-cm, the experimental set described in Ref. 20 was used. For other values of fd, existing data summarized in Table 2 (Refs. 32–34) were used. The extrapolated curves were drawn using the results in Ref. 27 as a guide. It must be emphasized that Gould's results (Ref. 27) were computed and that they have not been verified experimentally. The range of experimental parameters in Fig. 21 is extensive. In comparison, fd varies from 20–2630 MHz-cm and breakdown voltages did not exceed a few hundred volts in the coaxial geometry.

Table 2. Experimental data

fd, MHz-cm	*f*, MHz	*d*, cms	Experimenter
38095	9400	4.05	McDonald, Gaskell, and Gitterman (Ref. 32)
18900	9400	2.01	
11812	9400	1.26	
4706	992	4.74	
3071	9400	0.327	
1966	992	1.98	
994	3125	0.318	Herlin and Brown (Ref. 33)
491	3125	0.157	
250	66.75	3.75	Woo
100	66.75	1.5	
50	66.75	0.75	
20	66.75	0.3	
10	200	0.05	Pim (Ref. 34)

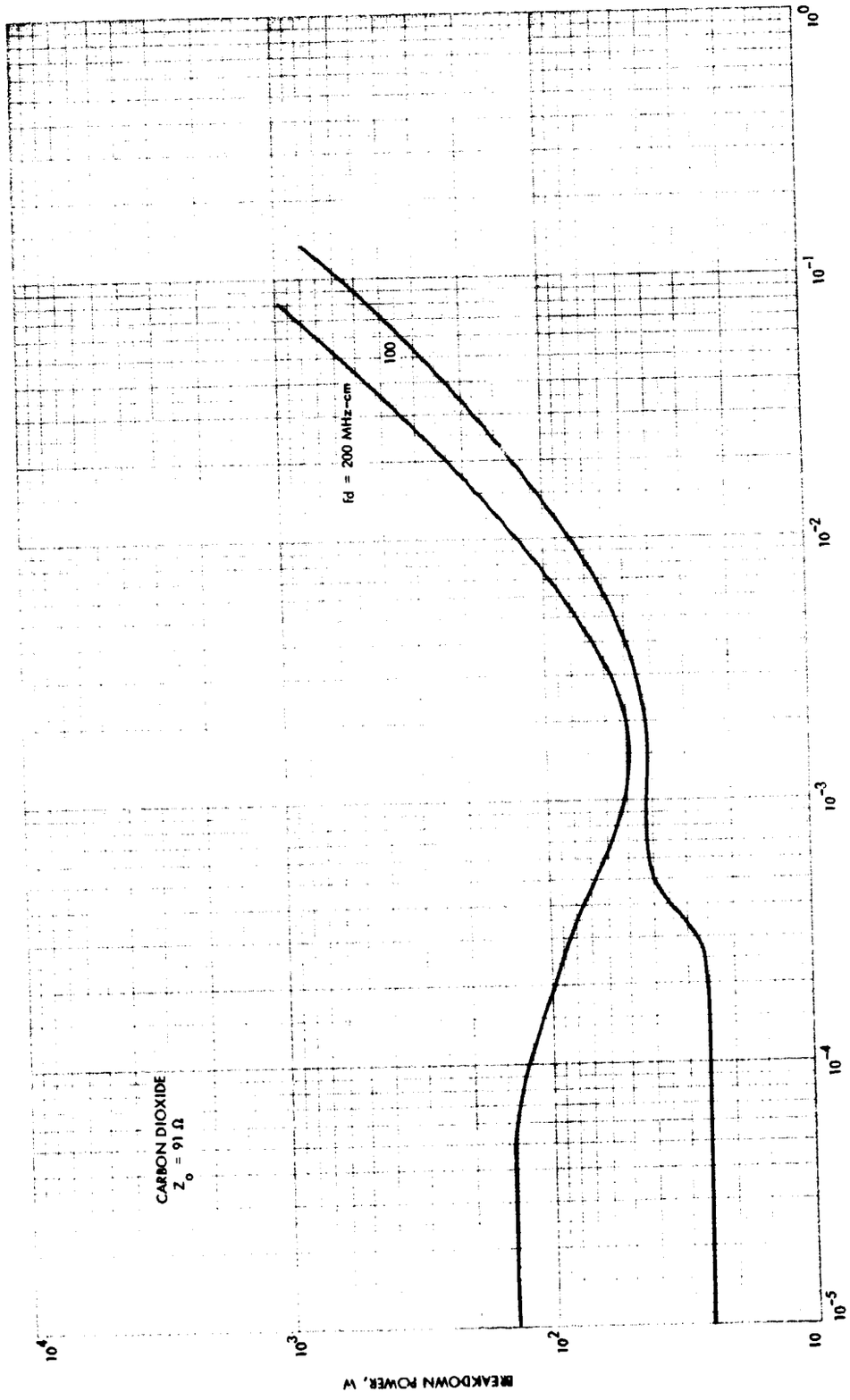

Fig. 19. Breakdown in carbon dioxide, Z_o = 91 Ω

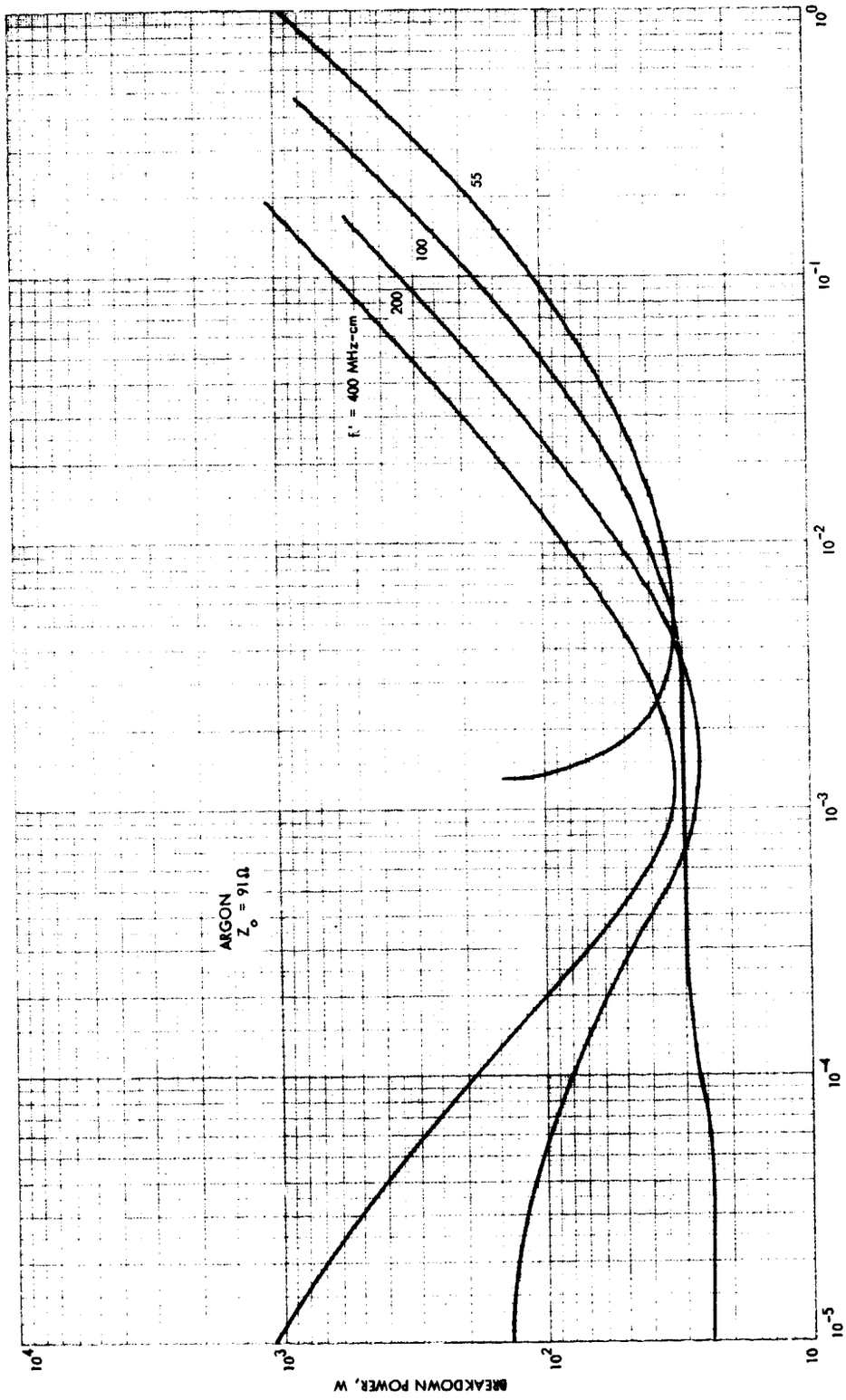

Fig. 20. Breakdown in argon, Z_o = 91 Ω

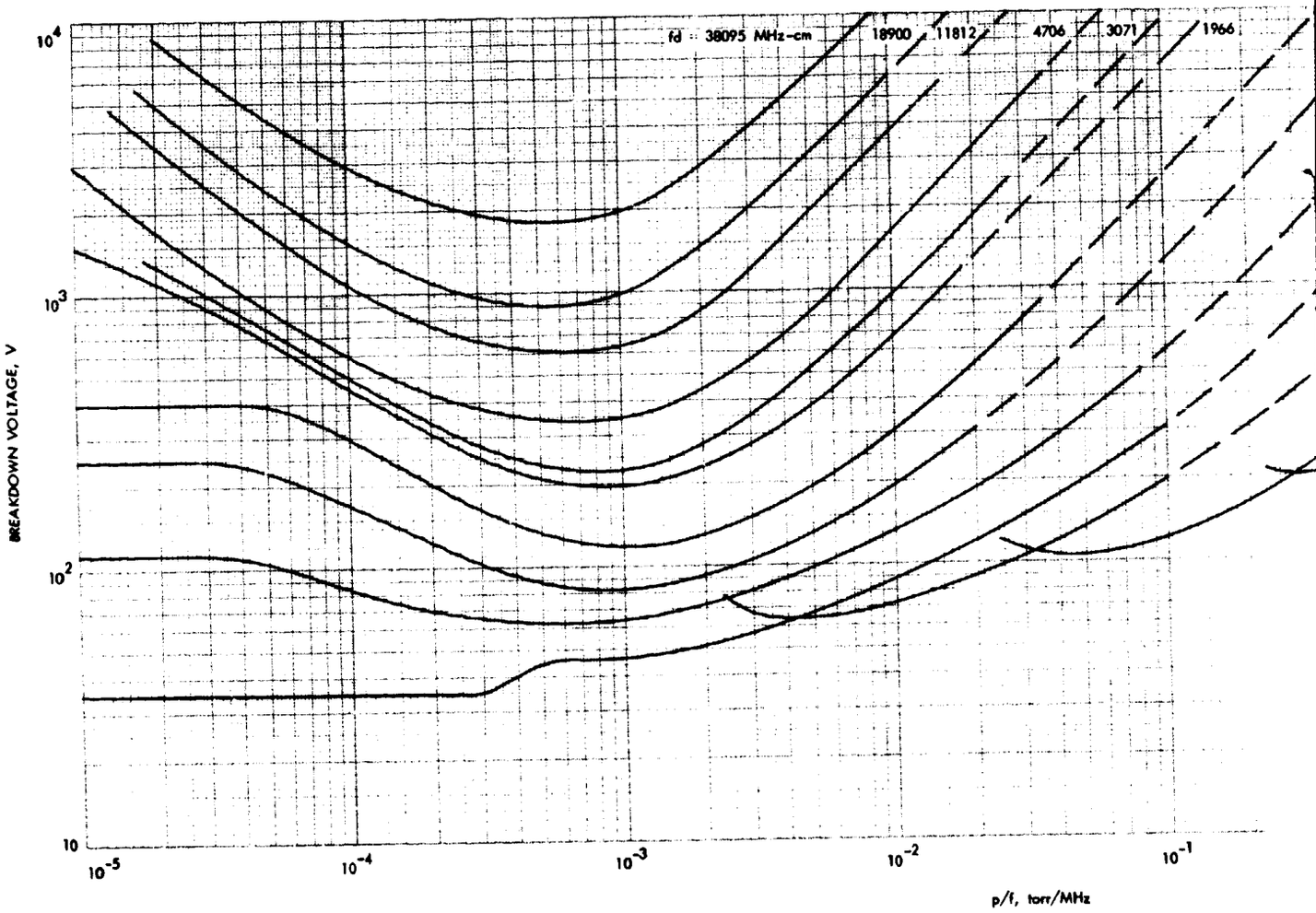

FOLDOUT FRAME 1

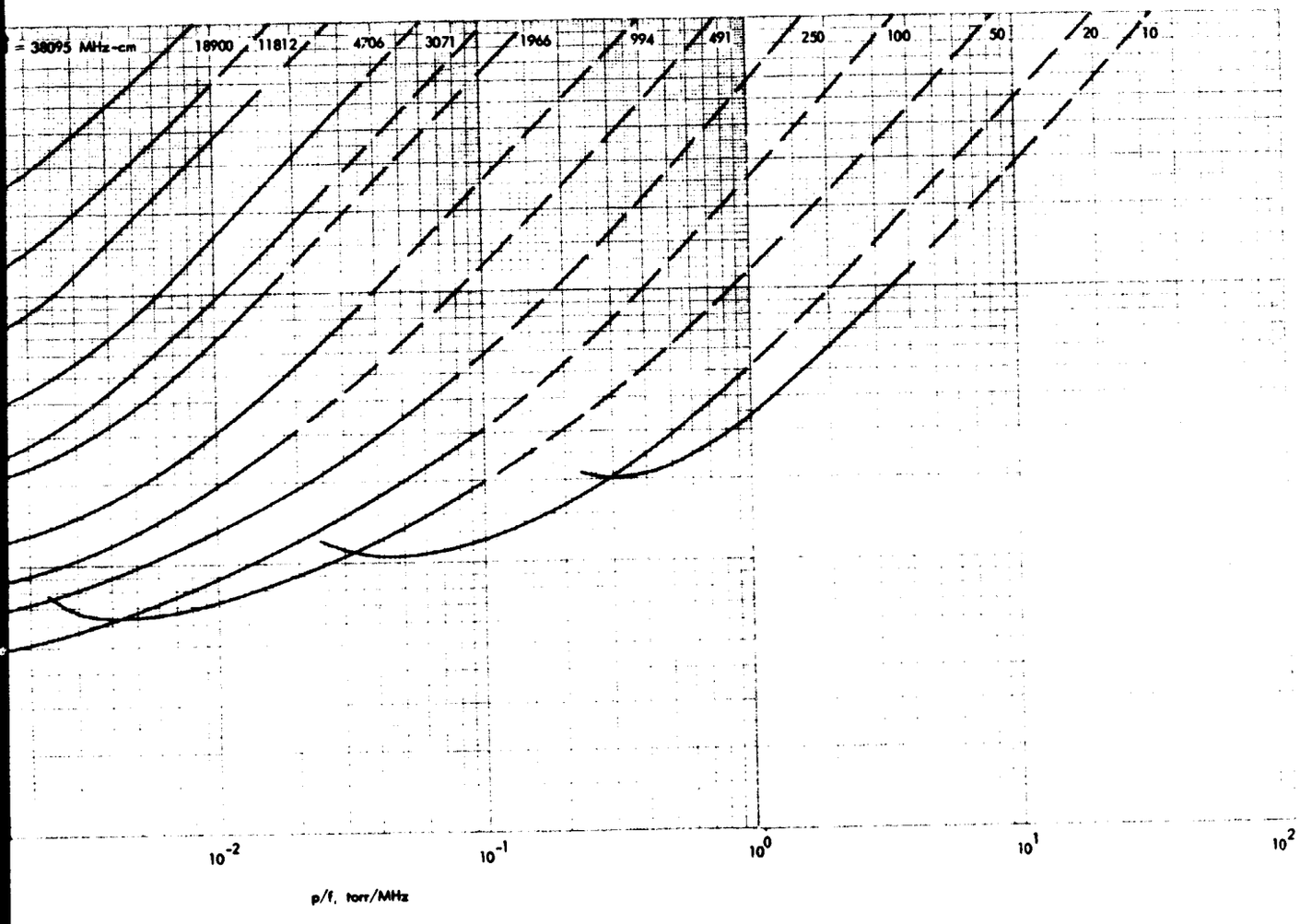

Fig. 21. RF voltage breakdown in uniform fields in air

FOLDOUT FRAME 2

As mentioned in Section IV-A, voltage breakdown problems were encountered in *Mariners VI* and *VII*. During ascent through the earth's atmosphere, both *Mariners VI* and *VII* experienced anomalous drops in signal transmission (Ref. 35). These anomalies disappeared as both spacecraft left the earth's atmosphere. It is suspected that ionization breakdown occurred in the RF switches and disappeared as the ambient pressure decreased. Fortunately, the RF power was relatively low (20 W) and the switches sustained no permanent damage. Serious damage would have resulted had the power been higher. Failures of the RF switches have shown up again in environmental tests for *Mariner 71*.* The usefulness of the type of data displayed in Fig. 21 was demonstrated in alleviating these problems. Using Fig. 21 as a guide, the switches were redesigned so that gap spaces within the range where breakdown could occur were excluded.

Atmospheric pressure is included in Fig. 21. This information is particularly useful when determining, for instance, the power limitations of the RF system at the Goldstone Space Communication Station. However, it should be pointed out that for many microwave components operating at atmospheric pressure, mechanical failure (such as melting) occurs at lower levels of RF power than voltage breakdown.

When breakdown is higher than 10^4 V the curves in Fig. 21 may still be used. For these cases, breakdown

*Private communication with Robert Hughes, Jet Propulsion Laboratory, Telecommunications Division, Pasadena, Calif.

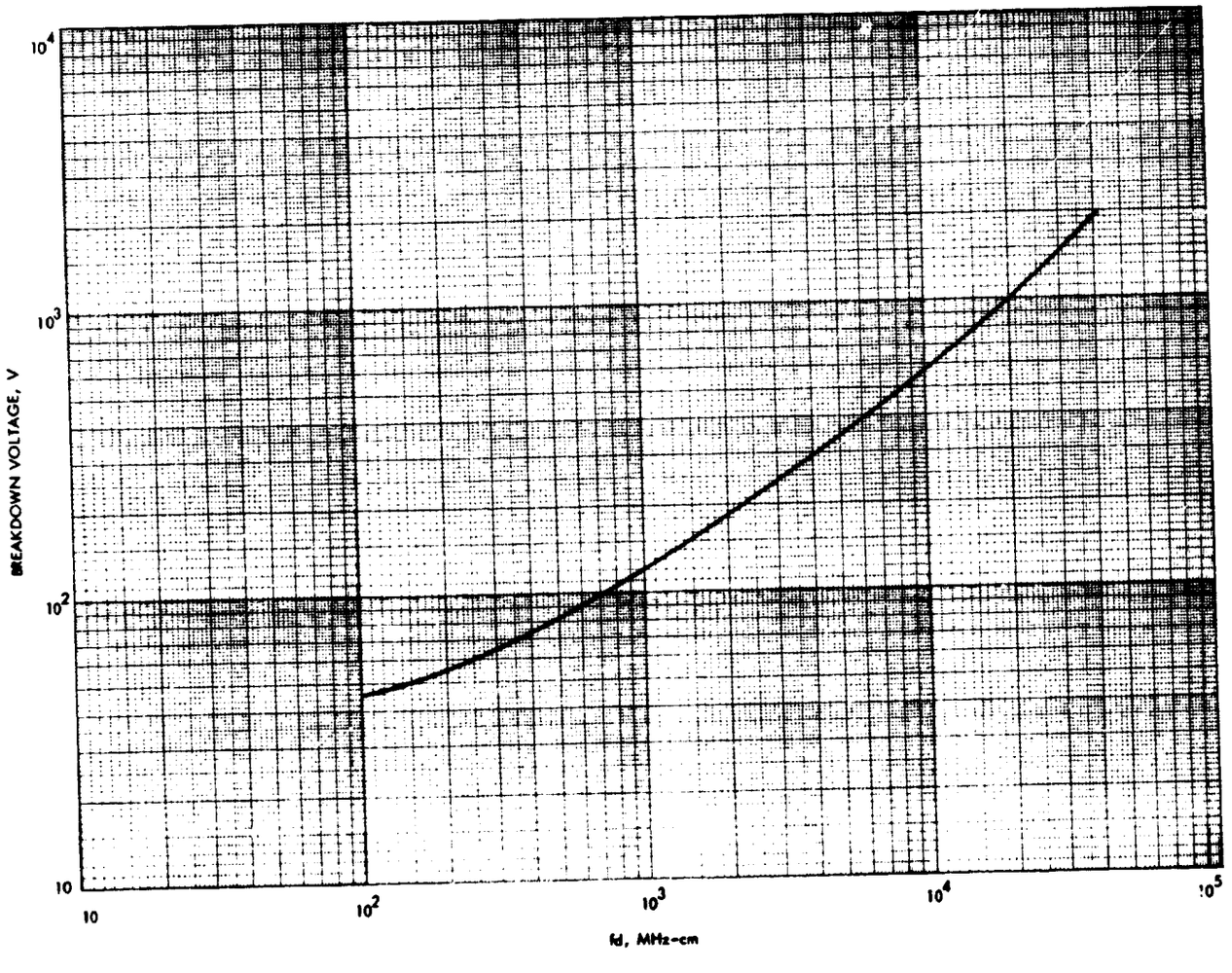

Fig. 22. Minimum ionization breakdown voltage as a function of *fd*

conditions are governed by attachment and breakdown voltage is simply proportional to pressure. Thus the curves can be extended by straight lines possessing a slope of 1.

Shown in Fig. 22 is the minimum ionization breakdown voltage as a function of fd, for fd values greater than 100 MHz-cm. Note from Fig. 5 that for $fd = 100$ MHz-cm, the voltage required for multipacting is lower than that for ionization breakdown.

V. Breakdown Prevention

Various techniques are available for preventing breakdown or improving power handling in RF coaxial transmission lines. It must be emphasized, however, that these techniques were not investigated in this study. The purpose of this section is merely to list the existing methods and offer some brief comments.

A. Configuration Change

Using the universal curves obtained in this report as a guide, frequency, line size, or characteristic impedance may be altered to improve power handling.

B. Use of Solid Dielectrics

A solid dielectric, such as Teflon, may be used to fill the interconductor air space either partially or completely. In the former case, a reduced air space could raise the power required for breakdown. In the latter case, dielectric failure is the limiting factor for power handling. Dielectric failure generally occurs at power levels considerably higher than those required for breakdown as discussed in this report. Therefore, filling the interconductor air space with a solid dielectric represents a sure way of preventing breakdown. The only disadvantage in this method is the high RF loss that results for high frequencies. Foam dielectrics do not appear desirable because of the existence of air cells (Ref. 3).

C. Pressurization

Appreciable improvement in power handling results from pressurization. The disadvantage in this method is the problem of reliability associated with long-term pressurization.

D. DC Bias

A dc bias can be applied across the inner and outer conductors. In many cases, the dc bias required may be fairly high.

E. Surface Treatment to Reduce Secondary Emission

This method applies to multipacting only. The idea is to reduce the secondary emission δ to less than unity so that multipacting will not occur. Deposition of titanium (Ref. 36) and carbon (Ref. 37) have both been investigated. Titanium has been used with some success in preventing multipacting in klystrons (Ref. 38). For components that are exposed to air, such as transmission lines, oxides of titanium are formed and the secondary emission δ increases above unity. Deposition of a thin carbon film does not reduce δ significantly below unity (Ref. 37). Thus, both types of surface treatment will not eliminate multipacting in coaxial transmission lines.

VI. Conclusions

Voltage breakdown in the RF coaxial transmission line has been studied in detail. The principle behind this investigation is similarity or scaling. The advantage of scaling is significant, since it allows universal curves to be constructed from a minimum of experimental data. These universal curves are simple to use and cover a wide range of experimental parameters. It is felt that these data are sufficient to determine the power handling capability of any coaxial transmission line likely to be encountered by a spacecraft design engineer. Although the data in this report are restricted to uniform and coaxial fields, they may be used to estimate breakdown levels in other configurations as well.

References

1. *The Lunar Program*, Space Program Summary 37-21, Vol. I, pp. 29–32. Jet Propulsion Laboratory, Pasadena, Calif., May 31, 1963.

2. Brunstein, S., "Radio Frequency Multipactor Voltage Breakdown on the Ranger Lunar Probe," in *Supporting Research and Advanced Development*, Space Program Summary 37-35, Vol. IV, p. 282. Jet Propulsion Laboratory, Pasadena, Calif., Oct. 31, 1965.

3. *Proceedings of the Workshop on Voltage Breakdown in Electronic Equipment at Low Air Pressures*. Edited by E. R. Bunker, Jr., Technical Memorandum 33-280. Jet Propulsion Laboratory, Pasadena, Calif., Dec. 15, 1966.
Also *Proceedings of the Second Workshop on Voltage Breakdown in Electronic Equipment at Low Air Pressure*. Edited by E. R. Bunker, Jr., Technical Memorandum 33-447. Jet Propulsion Laboratory, Pasadena, Calif., June 30, 1970.

4. Baller, H. H., and Phillips, E. V., *Investigations of Failures of Wideband OAO Transmitter in Vacuum Test*, TM-756. Hughes Aircraft Co., Culver City, Calif., July 1963.

5. *The Study of Multipactor Breakdown in Space Electronic Systems*, Report No. P65-49, Vols. I and II. Hughes Aircraft Co., Culver City, Calif., April 1965.

6. Meek, J. M., and Craggs, J. D., *Electrical Breakdown of Gases*. Clarendon Press, Oxford, London, 1953.

7. Brown, S. C., Basic Data of Plasma Physics. John Wiley & Sons, Inc., New York, 1959.

8. McDaniel, E. F., *Collision Phenomena in Ionized Gases*, John Wiley & Sons, Inc., New York, 1964.

9. Hatch, A. J., and Williams, H. B., "The Secondary Electron Resonance Mechanism of Low-Pressure High-Frequency Gas Breakdown," *J. Appl. Phys.*, Vol. 25, No. 4, pp. 417–423, April 1954.

10. Hatch, A. J., and Williams, H. B., "Multipacting Modes of High Frequency Gaseous Breakdown," *Phys. Rev.*, Vol. 112, No. 3, pp. 681–685, Nov. 1958.

11. Brown, S. C., "Breakdown in Gases: Alternating and High Frequency Fields," in *Handbuch der Physik*. Edited by S. Flugge. Springer-Verlag, Berlin, Vol. 22, pp. 531–575, 1956.

12. Francis, G., *Ionization Phenomena in Gases*, Butterworth's Scientific Publications, London, pp. 81–172, 1960.

13. MacDonald, A. D., *Microwave Breakdown in Gases*, John Wiley & Sons, Inc., New York, 1966.

14. Biondi, M. A., "Microwave Gas Discharges," *AIEE Trans.*, Vol. 69, pp. 808–809, Sept. 1950.

References (contd)

15. Prowse, W. A., "The Initiation of Breakdown in Gases Subject to High-Frequency Electric Fields," *J. of the British Inst. of Radio Engineers*, pp. 333–347, Nov. 1950.

16. Priest, D. H., and Talcott, R. C., "On the Heating of Output Windows of Microwave Tubes by Electron Bombardment," *IRE Trans. on Electron Devices*, pp. 243–251, July 1961.

17. Hatch, A. J., "Suppression of Multipacting in Particle Accelerators," *Nucl. Instrum. Methods*, No. 41, pp. 261–271, 1966.

18. Forrer, M. P., and Milazzo, "Duplexing and Switching with Multipactor Discharges," *Proc. of the IRE*, pp. 442–450, April 1962.

19. Vance, E. F., "One-Sided Multipactor Discharge Modes," *J. Appl. Phys.*, Vol. 34, No. 11, pp. 3237–3242, Nov. 1963.

20. Woo, R., "Multipacting Discharges Between Coaxial Electrodes," *J. Appl. Phys.*, Vol. 39, No. 3, pp. 1528–1533, Feb. 1968.

21. Callebaut, D. K., Verhaeghe, J. L., and Bouten, M. J., "Secondary Electron Resonance Discharge II, Steady State by Return," *Physica*, No. 30, pp. 825–847, 1964.

22. Woo, R., and Ishimaru, A., "A Similarity Principle for Multipacting Discharges," *J. Appl. Phys.*, Vol. 38, No. 13, pp. 5240–5244, Dec. 1967.

23. Callebaut, D. K., "Secondary Electron Resonance Discharge I. Steady State by Debunching," *Physica*, No. 29, pp. 784–802, 1963.

24. Woo, R., "Multipacting Breakdown in Coaxial Transmission Lines," *Proc. Inst. Elec. Eng.*, Vol. 56, No. 4, pp. 776–777, April 1968.

25. Woo, R., "Multipacting in Coaxial Geometries," in *Supporting Research and Advanced Development*, Space Program Summary 37-58, Vol. III, pp. 61–65. Jet Propulsion Laboratory, Pasadena, Calif., Oct. 31, 1969.

26. Herlin, M. A., and Brown, S. C., "Electrical Breakdown of a Gas Between Coaxial Cylinders at Microwave Frequencies," *Phys. Rev.*, Vol. 74, No. 8, pp. 910–913, Oct. 1948.

27. Gould, L., *Handbook on Breakdown of Air in Waveguide Systems*, Microwave Associates Report Index No. NE 111616, April 1956.

28. Woo, R., "RF Voltage Breakdown in Coaxial Transmission Lines," *Proc. Inst. Elec. Eng.*, Vol. 57, No. 2, pp. 254–256, Feb. 1969.

29. Brown, S. C., and MacDonald, A. D., "Limits for the Diffusion Theory of High Frequency Gas Discharge Breakdown," *Phys. Rev.*, Vol. 76, No. 11, pp. 1629–1633, Dec. 1949.

30. Anashkin, G. A., "Space-Charge Effects in a High Frequency Gas Discharge," *Sov. Phys.–Tech. Phys.*, Vol. 12, pp. 1076–1080, 1968.

31. Wheeler, H. A., *Nomograph for Some Limitations on High Frequency Voltage Breakdown in Air*, Wheeler Lab Report No. 17. Wheeler Laboratories, Great Neck, N.Y., May 1953.

References (contd)

32. MacDonald, A. D., Gaskell, D. U., and Gitterman, H. N., "Microwave Breakdown in Air, Oxygen, and Nitrogen," *Phys. Rev.*, Vol. 130, No. 5, pp. 1841–1850, June 1963.

33. Herlin, M. A., and Brown, S. C., "Breakdown of a Gas at Microwave Frequencies," *Phys. Rev.*, Vol. 74, No. 3, pp. 291–296, Aug. 1948.

34. Pim, J. A., "The Electrical Breakdown Strength of Air at Ultra-High Frequencies," *Proc. Inst. Elec. Eng.*, Vol. 96, Part III, pp. 117–129, 1949.

35. *Mariner 69 Final Report*, Vol. II. Jet Propulsion Laboratory, Pasadena, Calif. (to be published).

36. Talcott, R. C., "The Effects of Titanium Films on Secondary Electron Emission Phenomena in Resonant Cavities and at Dielectric Surfaces," *IRE Trans. Electron Devices*, Vol. 9, pp. 405–410, Sept. 1962.

37. Erpenbach, H., *Secondary Electron Emission and Means of Reducing the Yield*, Technical Memorandum 33-366. Jet Propulsion Laboratory, Pasadena, Calif., Nov. 15, 1967.

38. *Research on Microwave Window Multipactor and its Inhibition*, Final Report, Contract No. DA 36-039 SC-90818. Dept. of the Army, Eimac, San Carlos, Calif., 1964.